Neuropharmacology 149 (2019) 66–82

Contents lists available at ScienceDirect

Neuropharmacology

journal homepage: www.elsevier.com/locate/neuropharm

Developmental nicotine exposure precipitates multigenerational maternal transmission of nicotine preference and ADHD-like behavioral, rhythmometric, neuropharmacological, and epigenetic anomalies in adolescent mice

Jordan M. Buck[a,b,*], Kelsey N. Sanders[a], Charles R. Wageman[a], Valerie S. Knopik[c], Jerry A. Stitzel[a,b], Heidi C. O'Neill[a]

[a] Institute for Behavioral Genetics, University of Colorado, Boulder, United States
[b] Department of Integrative Physiology, University of Colorado, Boulder, United States
[c] Department of Human Development and Family Studies, Purdue University, United States

HIGHLIGHTS

- Developmental nicotine exposure elicits multigenerational nicotine preference.
- Developmental nicotine exposure causes multigenerational hyperactivity/risk-taking.
- Developmental nicotine exposure causes multigenerational rhythmometric aberrations.
- Developmental nicotine exposure causes multigenerational corticostriatal anomalies.
- Developmental nicotine exposure produces multigenerational DNA methylome deficits.

ARTICLE INFO

Keywords:
Nicotine
Development
ADHD
Dopamine
Acetylcholine
Methylation

ABSTRACT

Maternal smoking during pregnancy, a form of developmental nicotine exposure (DNE), is associated with increased nicotine use and neurodevelopmental disorders such as ADHD in children. Here, we characterize the behavioral, rhythmometric, neuropharmacological, and epigenetic consequences of DNE in the F1 (first) and F2 (second) generation adolescent offspring of mice exposed to nicotine prior to and throughout breeding. We assessed the effects of passive oral methylphenidate (MPH) administration and voluntary nicotine consumption on home cage activity rhythms and activity and risk-taking behaviors in the open field. Results imply a multigenerational predisposition to nicotine consumption in DNE mice and demonstrate ADHD-like diurnal and nocturnal hyperactivity and anomalies in the rhythmicity of home cage activity that are reversibly rescued by MPH and modulated by voluntary nicotine consumption. DNE mice are hyperactive in the open field and display increased risk-taking behaviors that are normalized by MPH. Pharmacological characterization of nicotinic and dopaminergic systems in striatum and frontal cortex reveals altered expression and dysfunction of nicotinic acetylcholine receptors (nAChRs), hypersensitivity to nicotine-induced nAChR-mediated dopamine release, and impaired dopamine transporter (DAT) function in DNE mice. Global DNA methylation assays indicate DNA methylome deficits in striatum and frontal cortex of DNE mice. Collectively, our data demonstrate that DNE enhances nicotine preference, elicits hyperactivity and risk-taking behaviors, perturbs the rhythmicity of activity, alters nAChR expression and function, impairs DAT function, and causes DNA hypomethylation in striatum and frontal cortex of both first and second-generation adolescent offspring. These findings recapitulate multiple domains of ADHD symptomatology.

* Corresponding author. Institute for Behavioral Genetics, University of Colorado Boulder, 1480 30th Street, Boulder, CO, 80309-0447, United States.
E-mail address: Jordan.Buck@colorado.edu (J.M. Buck).

https://doi.org/10.1016/j.neuropharm.2019.02.006
Received 16 May 2018; Received in revised form 11 January 2019; Accepted 4 February 2019
Available online 08 February 2019
0028-3908/

1. Introduction

Approximately 10% of women in the U.S. report smoking during pregnancy, which is associated with numerous fetal consequences including premature birth, low birth weight, and Sudden Infant Death Syndrome (SIDS) (Centers for Disease Control and Prevention, 2011; Salihu and Wilson, 2007; Knopik et al., 2016a). Developmental nicotine exposure (DNE) via maternal smoking during pregnancy is also associated with neurodevelopmental disorders such as conduct disorder (CD), substance use disorders (SUDs), and attention-deficit/hyperactivity disorder (ADHD) (Ernst et al., 2001; Linnet et al., 2003; Button et al., 2007; Knopik, 2009; Centers for Disease Control and Prevention, 2011; Knopik et al., 2016b; He et al., 2017; Huang et al., 2018; Marceau et al., 2018). Importantly, children of maternal smokers are more likely to smoke, initiate smoking earlier, and smoke more (Cornelius et al., 2000; Ernst et al., 2001; Buka et al., 2003; Agrawal et al., 2010; Centers for Disease Control and Prevention, 2011). Similarly, studies in mice have shown hyperactivity (Ajarem and Ahmad, 1998; Pauly et al., 2004; Paz et al., 2007; Heath et al., 2010; Zhu et al., 2012), reduced nicotine sensitivity (Pauly et al., 2004), and increased nicotine self-administration (Chistyakov et al., 2010) in adolescent DNE offspring.

Approximately 10% of children in the U.S. are diagnosed with ADHD (National Survey of Children's Health, 2011–2012), a neurodevelopmental disorder characterized by inattention, impulsivity, and hyperactivity (American Psychiatric Association, 2013). In addition, ADHD patients exhibit diurnal and nocturnal hyperactivity and sleep disturbances, increased amplitude of rest-wake activity rhythms, phase-delayed rest-wake activity rhythms (late chronotype or eveningness), phase-delayed cortisol and melatonin rhythms, and arrhythmicity of the biological clock proteins BMAL1 and PER2 (Baird et al., 2012; Van Veen et al., 2010; Imeraj et al., 2012; Bijlenga et al., 2013; Snitselaar et al., 2017). Psychostimulant treatment of ADHD patients attenuates hyperactivity and exerts phase-shifting effects on circadian rest-activity rhythms (Snitselaar et al., 2017). Analogous to the children of maternal smokers, adolescent ADHD patients are more likely to smoke (Kollins et al., 2005), initiate smoking earlier (Milberger et al., 1997; Elkins et al., 2018) and are more likely to escalate to daily smoking (Lambert and Hartsough, 1998; Rhodes et al., 2016). Moreover, nicotine-dependent adolescent ADHD patients experience exacerbated withdrawal symptoms (Gray et al., 2010; Bidwell et al., 2018). The self-medication hypothesis of the co-morbidity of ADHD and smoking suggests that the increased risk for nicotine dependence in ADHD patients is mediated by a therapeutic effect of nicotine (Amsterdam et al., 2018). Consistent with this hypothesis, nicotine and other nicotinic compounds have clinical efficacy in treating inattention, impulsivity, and hyperactivity in ADHD patients (Gehricke et al., 2009). In addition, research has identified an association between smoking and late chronotype such as that observed in ADHD patients (Wittmann et al., 2006). Interestingly, nicotine phase-advances the firing rhythms of suprachiasmatic nucleus (SCN) neurons that control the circadian clock (Logan et al., 2014) and that appear to be phase-delayed in ADHD patients exhibiting a late chronotype (Baird et al., 2012; Bijlenga et al., 2013).

Expression of nAChRs during fetal development is spatiotemporally regulated and is an integral mediator of differentiation and synaptogenesis in the developing brain (Hellstrom-Lindahl et al., 1998; Cairns and Wonnacott, 1988; Agulhon et al., 1999; Falk et al., 2005; Abreu-Villaca et al., 2011). *In utero* nicotine exposure atemporally stimulates nAChRs and prematurely induces neuronal differentiation, leading to neuronal loss and impaired neurodevelopment in nAChR-expressing circuits such as the corticostriatothalamic dopamine (DA) network (Slotkin et al., 1987; Slotkin, 2002; Smith et al., 2010). Similarly, DNE results in immature prefrontal cortical development and reduced nicotinic acetylcholine receptor (nAChR) currents (Bailey et al., 2014). Prenatal nicotine exposure decreases DA release and turnover and tyrosine hydroxylase (TH) immunoreactivity in the prefrontal cortex and neofrontal cortex of F1 offspring mice (Muneoka et al., 1999; Alkam et al., 2017). Analogous to findings in the frontal cortex, deficits in striatal TH, DA, and brain-derived neurotrophic factor (BDNF) content are elicited by gestational nicotine exposure (Yochum et al., 2014). Many of the aforementioned DNE-induced brain changes mirror those observed in children with ADHD (Heath and Picciotto, 2009). For instance, impaired corticostriatothalamic DA signaling, which can result from DNE (Heath and Picciotto, 2009; Yochum et al., 2014), is implicated in ADHD (Del Campo et al., 2011) and is targeted by psychostimulant treatments for ADHD such as methylphenidate (MPH) (Volkow et al., 2001).

Contemporary research suggests a role for epigenetic changes in the neuropathology of ADHD. For instance, DNA methylation levels at birth are negatively correlated with symptom severity in children diagnosed with ADHD (van Mil et al., 2014). Perturbed DNA methylation patterns may represent a mechanistic basis for developmental deficits in prenatal nicotine-exposed children (for a review, see Knopik et al., 2018). Therein, maternal smoking during pregnancy is linked to persistent global and gene-specific DNA methylome aberrations in ADHD-relevant offspring brain regions such as the dorsolateral prefrontal cortex, as well as in fetal cord blood, that are associated with impaired neuronal differentiation and altered neuronal structure and synaptogenesis (Guerrero-Preston et al., 2010; Joubert et al., 2012; Richmond et al., 2015; Jung et al., 2016; Chatterton et al., 2017). Similarly, studies have shown persistent DNA methylome alterations in the placenta and children of maternal smokers that are enriched in pathways implicated in ADHD such as the processes of neuronal differentiation, development, and proliferation as well as synaptogenesis (Maccani and Maccani, 2015; Joubert et al., 2016).

Despite contemporary findings that DNE is associated with ADHD and impacts behavior, neurochemistry, and the epigenome, whether any such consequences of DNE are transmitted to subsequent generations remains largely unexplored. To address this void in the literature, the present study characterized the multigenerational effects of DNE on ADHD-relevant outcome measures including locomotor activity, risk-taking behaviors, nicotine consumption, nAChR expression and function in striatum and frontal cortex, and DNA methylation in striatum and frontal cortex. In addition, the multigenerational impacts of DNE on the rhythmicity of home cage activity, behavioral responses to methylphenidate treatment, and behavioral effects of nicotine consumption were evaluated to provide a more comprehensive profile of ADHD-relevant phenotypes and to better assess the construct validity and ADHD specificity of our DNE mouse model of ADHD.

2. Materials & methods

2.1. Reagents

(-)-Nicotine bitartrate, nicotine freebase, acetylcholine (ACh) iodide, diisopropyl fluorophosphate (DFP), NaCl, KCl, $CaCl_2$, $MgSO_4$, glucose, sucrose, HEPES, tetrodotoxin, polyethelenimine, bovine serum albumin (BSA), and cytisine were purchased from Sigma-Aldrich Chemical Co (St. Louis, MO). The radioisotopes [^{3}H]-dopamine (7,8-^{3}H at 20–40 Ci/mmol), carrier-free ^{86}RbCl (initial specific activity 13.6–18.5 Ci/μg), and [^{125}I]-epibatidine (2200 Ci/mmol) were purchased from Perkin Elmer (Waltham, MA). α-Conotoxin MII (α-CtxMII) was generously provided by J. Michael McIntosh, University of Utah, Salt Lake City, UT.

2.2. Animals

All experimental and housing conditions were reviewed and pre-approved by the Institutional Animal Care and Utilization Committee at the University of Colorado, Boulder, and conform to the guidelines for animal care and use established by the NIH and the Guide for the Care and Use of Laboratory Animals (8th Ed.). Mice were maintained on a standard 12 h light/dark cycle (lights on at 7:00 a.m.) and were

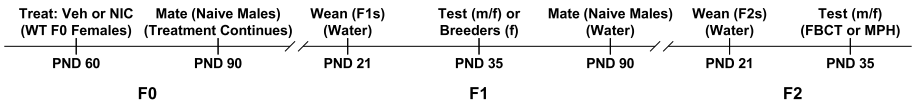

Fig. 1. Procedural Schematic for breeding and behavioral testing. Female C57BL/6J breeders were exposed to 0.2% saccharin (Veh) or 0.2% saccharin and nicotine (200 μg/mL) in drinking water for 30 days prior to mating with drug-naïve males. Veh or nicotine treatment of breeders continued until weaning of offspring at PND 21, after which water was provided to all offspring as the sole fluid source. Randomly selected F1 female developmental nicotine-exposed offspring were subsequently mated with drug-naïve male sires to obtain F2 generation maternal germline nicotine-exposed offspring. PND: post-natal day; Veh: 0.2% aqueous saccharin; nicotine: 200 μg/mL aqueous nicotine; F1 Veh: first-generation parental Veh-exposed offspring; F1 NIC: first-generation parental nicotine-exposed offspring; F2 NIC: second-generation parental nicotine-exposed offspring; four-bottle choice test: four-bottle choice test for voluntary oral nicotine intake and preference; MPH: passive oral methylphenidate treatment.

provided food (Envigo Teklad 2914 irradiated rodent diet, Harlan, Madison, WI) and water *ad libitum*. Thirty days prior to mating with drug-naïve males, female C57BL/6J (inbred strain) breeders received 0.2% saccharin (Veh) or 0.2% saccharin and nicotine (200 μg/mL) (DNE progeny) in place of water. Solutions were replaced twice weekly. Vehicle or nicotine treatment of breeders continued until weaning of offspring at PND 21, after which water was provided to all offspring as the sole fluid source. Randomly selected F1 female DNE offspring were subsequently mated with drug-naïve male sires to obtain F2 generation maternal germline nicotine-exposed offspring (Fig. 1). Female F1 DNE mice used for breeding of F2 generation progeny were naïve to both behavioral testing and direct (post-weaning) exposure to nicotine. Pilot experiments indicated no differences between F1 and F2 generation adolescent offspring of mice exposed to saccharin or plain water vehicle, and we thus elected to test only F1 developmental vehicle-exposed mice as DNE-naïve controls. Since drug-naïve male sires of F1 DNE mice were able to consume nicotine once co-housed with pre-treated females, this paradigm constitutes parental rather than exclusively maternal nicotine exposure. However, transmission of DNE-induced phenotypes from F1 to F2 generation offspring occurs exclusively via the F1 maternal germline/lineage. There were no group differences in litter size or pup survival rates. Behavioral testing was conducted beginning at PND 35 (early adolescence), and all molecular experiments utilized tissue collected at PND 45 (adolescence). All mice were bred in the same on-site animal facility. Both sexes of offspring were tested in all behavioral and molecular experiments. To control for between-litter and between-breeder variability within each group, a minimum of 15 total litters from a minimum of 12 total breeder pairs were behaviorally tested for each group.

For both passive oral methylphenidate (MPH) administration and the four-bottle choice test (four-bottle choice test), solutions were provided in Pyrex test tubes (9820, 18 mm × 150 mm, Fisher Scientific) fitted with rubber septa (Suba-Seal septa 29; Sigma Aldrich) containing a standard 6.5 cm stainless steel sipper tube. To permit concurrent top-down activity monitoring, MPH or nicotine bottles were loaded into equidistant holes drilled in the sides of standard polycarbonate home cages, and food was placed directly in the cage bottom. Separate cohorts of mice were utilized for MPH treatment, four-bottle choice test testing, and EZM testing. MPH treatment and four-bottle choice test testing were conducted using a within-subjects design. [^{125}I]-Epibatidine binding, [^{3}H]-dopamine ([^{3}H]-DA) release, and $^{86}Rb^{+}$ efflux assays were conducted using samples from a separate cohort of mice that were naïve to behavioral testing. [^{3}H]-DA uptake assays were performed using an additional separate cohort of mice that were naïve to behavioral testing.

2.3. Passive oral methylphenidate administration

To mimic treatment regimens in human ADHD patients, D,L-methylphenidate hydrochloride (MPH) (Sigma Aldrich, St. Louis, MO) was diluted in water to a concentration of 10 μg/mL and provided as the sole source of fluids during the dark (active) phase, while water was provided as the exclusive source of fluids during the light (inactive) phase. The 10 μg/mL MPH concentration used was selected based on average daily fluid consumption for all mice (4.23 mL/day) and the therapeutically-relevant dose range of 0.75–2 mg/kg/day, which previous research has translated from humans to mice (Balcioglu et al., 2009; Zhu et al., 2012, 2017).

2.4. Four-bottle choice test for nicotine intake and preference

The four-bottle choice test was conducted as previously described (Li et al., 2007) and adapted to enable concurrent home cage activity monitoring. We concurrently assessed nicotine intake and preference at 0, 25, 50, 100 μg/mL nicotine concentrations over two continuous four-day intervals. Bottles containing water or 25, 50, 100 μg/mL nicotine were weighed prior to and following days 1–4 of voluntary nicotine consumption and days 5–8 of voluntary nicotine consumption and were rotated daily to control for position bias. Daily nicotine consumption (mg/kg/day) served as the outcome measure for voluntary nicotine intake, and preference ratios (volume consumed from each bottle divided by the total daily fluid consumed) were calculated as the outcome measure for nicotine preference.

2.5. Passive home cage activity monitoring

Home cage locomotor activity of singly-housed mice was continuously monitored during each experimental stage, including a 3d baseline period, throughout MPH treatment and four-bottle choice test testing, over 4d following the conclusion of MPH treatment, and for a 24 h nicotine withdrawal period using cage top-mounted infrared motion sensors and VitalView Data Acquisition software (Starr Life Sciences Corporation, Oakmont, PA). Activity counts per day (separated by active and inactive phase) served as the dependent variable for passive home cage activity monitoring. In addition to summary measures of activity, rhythmometric analyses were performed to probe for potential ADHD-like alterations in the home cage activity rhythms of DNE mice. A detailed description of the rhythmometric analyses and parameters of rhythm is provided in the supplement (Fig. S3).

2.6. Open field testing

Locomotor activity and anxiety-like/risk-taking behaviors were assessed in 15-min open field trials conducted at baseline, immediately following MPH administration or the four-bottle choice test, following 24 h post-four-bottle choice test nicotine withdrawal, and 4d after the conclusion of MPH administration. Open field experiments were conducted in a 40 × 40 cm opaque plexiglass arena. Data were collected and processed using Activity Monitor (Med Associates Inc., Fairfax, VT). The center of the open field was defined as the inner 30 × 30 cm area, and the periphery as the residual 10 × 10 cm area. Total distance moved in the open field served as the outcome measure for locomotor activity in a novel environment. Since there were group differences in total distance moved, percent distance moved in the center of the open field was reported as the primary outcome measure for anxiety-like/risk-taking behaviors. An increase in percent distance moved in the center of the open field was interpreted as an increase in risk-taking behaviors, while a decrease in percent distance moved in the center of the open field was interpreted as a decrease in risk-taking behaviors. For all mice tested in the open field, measures of percent time spent in

the center of the open field were highly consistent with those for percent distance moved in the center of the open field (data not shown, but are available upon request).

2.7. Elevated zero maze

The elevated zero maze (EZM) was utilized in conjunction with the open field to assess anxiety-like/risk-taking behaviors at baseline in a separate cohort of mice. All mice were placed in the same open sector to begin each five-minute experiment. Data were collected using a ZeroMaze Test Chamber (AccuScan Instruments, Inc., Columbus, OH), which consisted of a narrow circular corridor with a diameter of 40.5 cm, a corridor width of 10 cm, and a base height of 70.5 cm above floor-level. The EZM apparatus contained two oppositely-positioned closed-corridor sections with clear walls extending to a height of 30.5 cm above the circular corridor, along with two oppositely-positioned open-corridor sections which lacked walls. Percent time spent in the open area (open-corridor sections) of the EZM was calculated as a measure of anxiety-like/risk-taking behaviors. An increase in percent time spent in the open area of the EZM was interpreted as an increase in risk-taking behaviors, while a decrease in percent time spent in the open area was interpreted as a decrease in risk-taking behaviors.

2.8. Tissue preparation for functional assays and radioligand binding

Tissue preparation was conducted as previously described (Marks et al., 2010). Briefly, at PND 45, whole brains were removed following cervical dislocation and decapitation and each bilateral frontal cortex or bilateral striata was dissected in a chilled glass dish. Following dissection, samples were transferred to chilled, isotonic (0.32 M), buffered (5 mM HEPES, pH 7.5) sucrose solution and homogenized using a glass-Teflon homogenizer. Samples were then centrifuged at 12,000 × *g* for 10 min. The resulting crude synaptosomal pellet was resuspended and immediately assayed for function, and residual crude synaptosomes were stored at −20 °C for subsequent membrane binding assays. To prepare membranes for radioligand binding, samples were resuspended in chilled hypotonic buffer (NaCl, 14 mM; KCl, 0.15 mM; $CaCl_2$, 0.2 mM, $MgSO_4$, 0.1 mM; HEPES, 2.5 mM, pH 7.5), incubated for 10 min at 22 °C, centrifuged at 20,000 × *g* at 4 °C for 20 min, washed by cyclical re-suspension and centrifugation, and stored in buffer at −20 °C until assaying.

2.9. [^{125}I]-epibatidine binding to membrane homogenates

[^{125}I]-Epibatidine binding to membrane homogenates was measured to quantify nAChR expression in striatal and frontal cortical synaptosomal membranes as previously described. (Marks et al., 2004; Whiteaker et al., 2000). Briefly, washed, frozen membrane pellets were resuspended in hypotonic buffer and centrifuged at 20,000 × *g* for 20 min. Resulting pellets were then resuspended in chilled water to a volume adjusted such that less than 10% of the [^{125}I]-epibatidine was protein-bound. Samples containing 30 μL of binding buffer containing 200pM [^{125}I]-epibatidine were then incubated for 3 h at room temperature in 96-well polystyrene plates (with 1 mM nicotine added for non-specific binding), and subsequently diluted with 200 μL chilled wash buffer. Dilute samples were then filtered through glass fiber filters (top-MFS type B; bottom- Gelman A/E, Gelman, Ann Arbor, MI) treated with 0.5% polyethelenimine under a 0.2atm vacuum using an Inotech Cell Harvester (Inotech Systems, Rockville, MD) and then washed five times with chilled wash buffer. For quantification of cytisine-resistant binding in striatal and cortical synaptosomes, 50 nM cytisine was added to block [^{125}I]-epibatidine binding to cytisine-sensitive (α4β2-containing, α4β2*-containing) nAChR binding sites (Grady et al., 2009; Marks et al., 2007). To isolate α-CtxMII-resistant binding sites in striatal synaptosomes, α-CtxMII (50 nM) was applied to block [^{125}I]-epibatidine binding to α-CtxMII-sensitive (α6β2-containing, α6β2* nAChR) binding sites as previously described (Grady et al., 2007, 2010; Salminen et al., 2004, 2007). Radioactivity was subsequently measured (at 80% efficiency) using a Packard Cobra Auto Gamma Counter (Packard Instruments, Downers Grove, IL), and total protein concentration was measured via a Bicinchonicic Acid (BCA) assay (Pierce, Thermo Scientific, Watham, MA).

2.10. Synaptosomal DA release

[^{3}H]-DA release from crude striatal synaptosomes was assayed as previously described. (Grady et al., 2007, 2010; Salminen et al., 2004, 2007). Briefly, synaptosomes were suspended in uptake buffer (NaCl, 128 mM; KCl, 2.4 mM; $CaCl_2$, 3.2 mM; KH_2PO_4, 1.2 mM; $MgSO_4$, 1.2 mM; HEPES, 25 mM (pH 7.5); glucose, 10 mM; ascorbic acid, 1 mM; pargyline, 0.01 mM) and incubated at 37 °C for 10 min prior to the addition of 100 nM [^{3}H]-DA (1 μCi per 0.20 mL synaptosomes), followed by an additional 5-min incubation at 37 °C. All subsequent procedures were conducted at room temperature. Synaptosomal aliquots of 80 μL were loaded onto glass fiber filters and superfused with uptake buffer to which was added 0.1% bovine serum albumin, 1 μM nomifensine, and 1 μM atropine at a flow rate of 0.7 mL/min for 10 min prior to fraction collection. To inhibit α6β2* nAChRs, a fraction of synaptosomal aliquots were exposed to α-CtxMII (50 nM) for the concluding 5 min of buffer superfusion. Following superfusion, DA release was stimulated via 20-s pulses of nicotine (0.01–30 μM), and fractions were collected into 96-well plates (Gilson FC204 fraction collector; Gilson, Inc., Middleton, WI) in 10-s intervals. Following addition of 0.15 mL OptiPhase SuperMix scintillation cocktail (Perkin-Elmer, Waltham MA), radioactivity was quantified using a 1450 Microbeta Trilux scintillation counter (Perkin-Elmer Life Sciences, Waltham, MA), with instrument efficiency of 40%. To isolate fractions of α6β2* nAChRs (MII-sensitive) and non-α6 containing (MII-resistant) nAChRs, the difference between α-CtxMII resistant DA release and total DA release was calculated.

2.11. Synaptosomal ^{86}Rubidium$^+$ efflux

Agonist-stimulated ^{86}Rubidium$^+$ (^{86}Rb$^+$) efflux from crude frontal cortical synaptosomes was assayed as previously described (Marks et al., 1999, 2004, 2007, 2010). Briefly, crude synaptosomes were resuspended in uptake buffer (NaCl, 140 mM; KCl, 1.5 mM, CaCl2, 2 mM; MgSO4, 1 mM; HEPES, 25 mM; glucose, 20 mM; pH 7.5) containing 4 μCi ^{86}RbCl and incubated for 30 min at 22 °C. To inhibit acetylcholinesterase, 10 μM diisopropyl fluorophosphate was added five minutes prior to the conclusion of incubation. Samples were subsequently filtered using 6 mm glass fiber filters (Type A/E, Gelman, Ann Arbor, MI) and were then washed with perfusion buffer [NaCl, 135 mM; CsCl, 5 mM; KCl, 1.5 mM; CaCl2, 2 mM; MgSO4, 1 mM; HEPES, 25 mM; glucose, 20 mM; tetrodotoxin, 50 nM; atropine 1 μM; bovine serum albumin (fraction V), 0.1%; pH 7.5]. Following washout, samples were exposed to increasing ACh concentrations (0.1, 0.3, 1, 3, 10, 30, 100, 300, and 1000 μM) for 5 s to evoke nAChR-mediated ^{86}Rb$^+$ efflux. To continuously measure ^{86}Rb$^+$ efflux, sample effluents were propelled through a 200 μL flow-through Cherenkov cell in a β -RAM Radioactivity HPLC Detector (IN/US Systems, Inc., Tampa, FL). Remaining synaptosomal preparations were stored in buffer at −20 °C for complementary [^{125}I]-epibatidine binding assays.

2.12. [^{3}H]-dopamine uptake

Striatal and frontal cortical synaptosomes were prepared and assayed as previously described (Grady et al., 1992). Briefly, synaptosomal preparations were resuspended in uptake buffer (128 mM NaCl, 2.4 mM KCl, 3.2 mM CaCl2, 1.2 mM KH2PO4, 1.2 mM MgSO4, 25 mM pH 7.0 HEPES, 10 mM glucose, 1 mM ascorbic acid, and 0.01 mM pargyline) and loaded onto 96 well plates (50μL/well) in quadruplicate,

and 100 µL uptake buffer and either 0.05 (approximate K_m for DAT-mediated DA uptake) or 1.0 µM (approximately 20× K_m for DAT-mediated DA uptake) [^{3}H]-DA (30–55 Ci/mmol with necessary volume of unlabeled DA to attain target concentration) was subsequently added to each well (Drenan et al., 2010). To isolate DA transporter (DAT)-mediated [^{3}H]-DA uptake, fluoxetine (200 nM) and desipramine (100 nM) were applied to block [^{3}H]-DA uptake via the serotonin transporter and norepinephrine transporter, respectively. Plate-loaded samples were incubated at 22 °C for 5 min (Jin et al., 2017). Nomifensine (500 µM) was used for blanks. Reactions were terminated via pass-filtration through an Inotech Cell Harvester (LabLogic Systems, Brandon, FL) onto dual-layer, uptake buffer-saturated sheets of GFA/E glass fiber filter (Gelman Sciences, Ann Arbor, MI) and GF/B glass fiber filter (Micro Filtration Systems, Dublin, CA) and samples were washed 4× in chilled uptake buffer. Following addition of 150 µL Ecoscint XR scintillation cocktail to each well (National Diagnostics, Atlanta, GA), radioactivity was quantified using a Wallac 1450 Microbeta scintillation counter (Perkin Elmer Life Sciences), with input counts measured by addition of 2 µL DA mix to separate wells. [^{3}H]-DA uptake (fmol/µg) was calculated by subtraction of blank CPM from sample CPM to yield CPM/fmol, and the resulting data were normalized to total protein concentration using a BCA assay (Pierce, Thermo Scientific, Watham, MA).

2.13. 5-methylcytosine global DNA methylation ELISA

Global 5-methylcytosine (5-mC) content in frontal cortex and striatum was quantified via enzyme-linked immunosorbent assay (ELISA) (Zymo Research Corp., Irvine, CA). Brains were collected following cervical dislocation at PND 45, and bilateral striata and frontal cortices were obtained by dissection on ice immediately following cervical dislocation and decapitation. Dissected samples were stored at −80 °C until assaying. 5-mC ELISAs were conducted in accordance with the manufacturer's protocol.

2.14. Statistical analyses

All datasets were screened for outliers using the ROUT test (Q = 1%), and confirmed outliers were excluded from subsequent analyses where appropriate. The number of outliers for each analysis is listed in the supplement (Table S1). A maximum of three outliers were excluded per group for each dataset. All data were initially analyzed by multifactoral ANOVA to determine if there were effects of sex, breeder, litter, season, or testing chamber. No main effects of or interactions with these factors were detected for any measure, so data were collapsed accordingly and further analyzed using the appropriate ANOVA or non-parametric test to assess the effects of DNE on outcome measures. Statistical analyses and data visualization were conducted using R (https://cran.r-project.org), SPSS (IBM Analytics, Armonk, NY), GraphPad Prism 7.04 (GraphPad Software, La Jolla, California, USA), and SigmaPlot Version 12 (Systat Software, Inc., San Jose, CA).

Baseline home cage locomotor activity data were analyzed by two-way repeated measures ANOVA with group (F1 $Veh_{n=61}$, F1 $NIC_{n=63}$, or F2 $NIC_{n=73}$) and phase (active or inactive) as factors. Datasets for total distance moved and percent distance moved in the center of the open field were analyzed by one-way ANOVA with group (F1 $Veh_{n=59}$, F1 $NIC_{n=52}$, or F2 $NIC_{n=71}$) as the sole factor. Data for percent time spent in the open arms of the elevated zero maze were analyzed by one-way ANOVA with group (F1 $Veh_{n=43}$, F1 $NIC_{n=17}$, or F2 $NIC_{n=31}$) as the sole factor. Where appropriate, Bonferroni's multiple comparisons post-hoc test was applied.

Data for NIC consumption in the four-bottle choice test were analyzed by one-way ANOVA with group (F1 $Veh_{n=38}$, F1 $NIC_{n=33}$, or F2 $NIC_{n=46}$) as the sole factor. Similarly, data for MPH consumption were analyzed by one-way ANOVA with group (F1 $Veh_{n=28}$, F1 $NIC_{n=24}$, or F2 $NIC_{n=31}$) as the sole factor. Where appropriate for each analysis, Bonferroni's multiple comparisons post-hoc test was applied.

To determine whether any behavioral effects of MPH or nicotine covaried with individual drug intake, home cage and open field data for MPH-treated and four-bottle choice-tested mice were transformed to percentage differences from baseline. These values were analyzed by three-way (home cage activity data) or two-way (open field and rhythmometric data) repeated measures ANCOVA with either MPH or nicotine intake as a covariate. Results indicated that the effects of MPH and nicotine on home cage activity, total distance moved in the open field, percent distance moved in the center of the open field, MESOR estimates, global amplitude estimates, and orthophase estimates did not significantly co-vary with individual MPH or nicotine intake (Table S2), indicating that the behavioral effects of either drug were not dose-dependent. Therefore, unprocessed (non-transformed) behavioral datasets for MPH-treated and four-bottle choice-tested mice were analyzed by the appropriate repeated measures ANOVA.

Home cage activity data for MPH-treated mice were analyzed by three-way repeated measures ANOVA with the factors group (F1 $Veh_{n=28}$, F1 $NIC_{n=24}$, or F2 $NIC_{n=31}$), phase (active or inactive phase), and experimental stage (BL, MPH, or post-MPH). Total distance moved and percent distance moved in the center of the open field for MPH-treated mice were analyzed by two-way repeated measures ANOVA with the factors group (F1 $Veh_{n=28}$, F1 $NIC_{n=24}$, or F2 $NIC_{n=31}$) and experimental stage (BL, MPH, or post-MPH). Where appropriate, Bonferroni's multiple comparisons post-hoc test was applied.

Home cage activity data for four-bottle choice-tested mice were analyzed by three-way repeated measures ANOVA with the factors group (F1 $Veh_{n=30}$, F1 $NIC_{n=32}$, or F2 $NIC_{n=33}$), phase (active or inactive phase), and experimental stage (BL, NIC1, NIC2, or WD). Total distance moved and percent distance moved in the center of the open field were analyzed by two-way repeated measures ANOVA with the factors group (F1 $Veh_{n=30}$, F1 $NIC_{n=24}$, or F2 $NIC_{n=35}$) and experimental stage (BL, NIC1, NIC2, or WD). Where appropriate, Bonferroni's multiple comparisons post-hoc test was applied.

Baseline rhythmometric datasets (MESOR, global amplitude, and orthophase) were analyzed by one-way ANOVA with group (F1 $Veh_{n=61}$, F1 $NIC_{n=63}$, or F2 $NIC_{n=73}$) as the sole factor. MESOR, global amplitude, and orthophase estimates for MPH-treated mice were analyzed by two-way repeated measures ANOVA with the factors group (F1 $Veh_{n=28}$, F1 $NIC_{n=24}$, or F2 $NIC_{n=31}$) and experimental stage (BL, MPH, or post-MPH). MESOR, global amplitude, and orthophase estimates for four-bottle choice-tested mice were analyzed by two-way repeated measures ANOVA with the factors group (F1 $Veh_{n=30}$, F1 $NIC_{n=32}$, or F2 $NIC_{n=33}$) and experimental stage (BL, NIC1, NIC2, or WD). Where appropriate, Bonferroni's multiple comparisons post-hoc test was applied.

Data for striatal nAChR binding were analyzed by one-way ANOVA with group (F1 $Veh_{n=12}$, F1 $NIC_{n=13}$, or F2 $NIC_{n=13}$) as the sole factor. Similarly, data for frontal cortical nAChR binding analyzed by one-way ANOVA with group (F1 $Veh_{n=12}$, F1 $NIC_{n=12}$, or F2 $NIC_{n=11}$) as the sole factor. Datasets for DAT-mediated [^{3}H]-DA uptake were also analyzed by one-way ANOVA with group (F1 $Veh_{n=4}$, F1 $NIC_{n=9}$, or F2 $NIC_{n=8}$) as the sole factor. Where appropriate for each analysis, Holm-Sidak's multiple comparisons post-hoc test was applied.

The impact of DNE on the concentration-response curve for nicotine-evoked [^{3}H]-DA release was calculated via least-squares non-linear regression using the Michaelis-Menten equation:

$$R = (R_{max})*[nicotine] / (EC_{50} + [nicotine])$$

Where R is nicotine-stimulated DA release at each nicotine concentration tested, R_{max} is the estimated maximal DA release, and EC_{50} is the estimated nicotine concentration ([nicotine]) eliciting half-maximal DA release (Grady et al., 2007, 2010; Salminen et al., 2004, 2007). Datasets for nAChR-mediated [^{3}H]-DA release were analyzed by one-way ANOVA with group (F1 $Veh_{n=18}$, F1 $NIC_{n=21}$, or F2 $NIC_{n=14}$) as the

sole factor, and, where appropriate, Holm-Sidak's multiple comparisons post-hoc test was applied.

The effect of DNE on ACh concentration ([Ach])–response relations measured by $^{86}Rb^+$ efflux was quantitated via least squares non-linear regression using a biphasic [agonist]-response model:

$$R_{ACh} = (R_{HS} * [ACh])/(EC_{HS} + [ACh]) + (R_{LS} * [ACh])/(EC_{LS} + [ACh])$$

Where R_{ACh} is ACh-evoked $^{86}Rb^+$ efflux at each ACh concentration tested, R_{HS} and R_{LS} are the estimated maximal rates of $^{86}Rb^+$ efflux with higher and lower sensitivity to ACh stimulation, and EC_{HS} and EC_{LS} are the estimated ACh concentrations eliciting half-maximal $^{86}Rb^+$ efflux with higher and lower sensitivity to ACh stimulation, respectively (Marks et al., 1999, 2004, 2007, 2010, 2012). Datasets for frontal cortical nAChR-mediated $^{86}Rb^+$ efflux were analyzed by one-way ANOVA with group (F1 $Veh_{n=12}$, F1 $NIC_{n=12}$, or F2 $NIC_{n=11}$) as the sole factor, and, where appropriate, Holm-Sidak's multiple comparisons post-hoc test was applied.

Datasets for 5-mC abundance were analyzed by one-way ANOVA with group (F1 $Veh_{n(FCX)=19;\ n(STR)=21}$, F1 $NIC_{n(FCX)=19;\ n(STR)=19}$, or F2 $NIC_{n(FCX)=16;\ n(STR)=20}$) as the sole factor, and, where appropriate, Holm-Sidak's multiple comparisons post-hoc test was applied.

3. Results

3.1. Impact of DNE on activity and risk-taking behaviors in F1 and F2 adolescent mice

The experimental procedures for the breeding of mice and the schedule of behavioral testing are depicted in Fig. 1 and detailed in the methods section. Briefly, F0 dams received either nicotine (200 μg/mL in 0.2% saccharin) or vehicle (0.2% saccharin) as the sole fluid source beginning 30 days prior to mating and continuing until the weaning of pups. F1 NIC mice were thereby exposed to vehicle and nicotine from conception until weaning, while F1 Veh mice were exposed to vehicle alone from conception until weaning. F2 NIC mice are the progeny of female F1 NIC mice mated with drug-naïve male sires. Aside from the oocytes from which they were conceived, F2 NIC mice were devoid of direct exposure to nicotine. All behavioral testing commenced at PND 35 (early adolescence), and all in-vitro assays utilized tissue obtained at PND 45 (adolescence).

The effect of DNE on baseline locomotor activity was assessed in a familiar (home cage) and novel (open field) environment. Baseline home cage locomotor activity data were analyzed by two-way ANOVA with group (F1 $Veh_{n=61}$, F1 $NIC_{n=63}$, or F2 $NIC_{n=73}$) and phase (active or inactive) as factors. Where appropriate, Bonferroni's multiple comparisons post-hoc test was applied. Main effects of group ($F_{2,385} = 42.56$; $p = 1e^{-13}$) and phase ($F_{1,385} = 1624$; $p = 1e^{-15}$) and a significant group × phase interaction ($F_{2,385} = 9.84$; $p = 0.00007$) were detected for baseline home cage activity. F1 NIC and F2 NIC mice were more active in both the active phase ($p = 1e^{-14}$ and $p = 2e^{-12}$, respectively) (Fig. 2A) and the inactive phase ($p = 0.0091$ and $p = 0.0088$, respectively) (Fig. 2B) compared to F1 Veh mice.

Datasets for total distance moved and percent distance moved in the center of the open field were analyzed by one-way ANOVA with group (F1 $Veh_{n=59}$, F1 $NIC_{n=52}$, or F2 $NIC_{n=71}$) as the sole factor. Data for percent time spent in the open arms of the elevated zero maze were analyzed by one-way ANOVA with group (F1 $Veh_{n=43}$, F1 $NIC_{n=17}$, or F2 $NIC_{n=31}$) as the sole factor. Where appropriate for either analysis, Bonferroni's multiple comparisons post-hoc test was applied. There were main effects of group on total distance moved and percent distance moved in the center of the open field ($F_{2,179} = 11.96$, $p = 0.00001$ and $F_{2,179} = 16.0$, $p = 4.04e^{-7}$, respectively). F1 NIC and F2 NIC mice moved a greater total distance in the open field ($p = 0.0039$ and $p = 0.00001$, respectively) (Fig. 2C) and moved a greater percent distance in the center ($p = 0.0007$ and $p = 3.56e^{-7}$, respectively) (Fig. 2D) compared to F1 Veh mice. Since distance moved in the center of the open field is thought to measure anxiety-like/risk-taking behaviors, a separate cohort of mice was evaluated for risk-taking behaviors in the elevated zero maze (EZM). A main effect of group was detected for percent time spent in the open quadrants of the EZM ($F_{2,87} = 14.5$; $p = 3.65e^{-6}$). F1 NIC and F2 NIC mice spent a greater percent time in the open quadrants of the EZM compared to F1 Veh mice ($p = 0.00001$ and $p = 0.0012$, respectively) (Fig. S1), indicating increased risk-taking in DNE mice.

3.2. Impact of DNE on voluntary nicotine intake and preference in F1 and F2 adolescent mice

The impact of DNE on voluntary oral nicotine intake and preference in adolescent mice was assessed using the four-bottle choice test. Nicotine consumption data were analyzed by one-way ANOVA with group (F1 $Veh_{n=38}$, F1 $NIC_{n=33}$, or F2 $NIC_{n=46}$) as the sole factor, and, where appropriate, Bonferroni's multiple comparisons post-hoc test was applied. ANOVA indicated a main effect of group ($F_{2,126} = 25.61$; $p = 4.63e^{-10}$) on average daily nicotine intake (Fig. 3A). Both F1 NIC and F2 NIC mice consumed more nicotine than F1 Veh ($p = 2.58e^{-10}$ and $p = 2.05e^{-5}$, respectively), and F1 NIC mice consumed more nicotine than F2 NIC ($p = 0.031$). In addition, a main effect of nicotine concentration ($F_{3,410} = 210.4$; $p = 3.42e^{-29}$) and a significant group x nicotine concentration interaction ($F_{6,410} = 53.48$; $p = 1.42e^{-48}$) were detected for nicotine preference ratios (Fig. 3B). F2 NIC mice consumed more 25μg/mL nicotine than F1 Veh and F1 NIC ($p = 3.59^{-6}$ and $p = 0.0014$, respectively), while F1 NIC and F2 NIC mice consumed more 50μg/mL nicotine than F1 Veh ($p = 0.00009$ and $p = 0.026$, respectively). F1 NIC mice consumed more 100μg/mL nicotine than F1 Veh and F2 NIC ($p = 0.00007$ and $p = 0.00027$, respectively). F1 Veh mice consumed more plain water (0μg/mL) than F1 NIC and F2 NIC mice ($p = 1.92e^{-15}$ and $p = 9.0e^{-14}$, respectively), and F2 NIC mice consumed more plain water than F1 NIC ($p = 0.030$). These data indicate that DNE leads to increased voluntary nicotine intake and preference for at least two generations. However, the manner in which F1 NIC and F2 NIC achieved higher nicotine intake varied based on nicotine concentration. Namely, F1 NIC mice exhibited essentially equal preference across all three nicotine concentrations provided, while F2 NIC mice preferred the lowest concentration tested (25μg/mL) and showed a F1 Veh-like aversion to the highest (100μg/mL) concentration.

3.3. Methylphenidate responsiveness of hyperactivity and risk-taking behaviors in DNE mice

To determine whether MPH could reduce or reverse the hyperactivity and risk-taking behaviors in DNE mice, home cage and open field activity were assessed before, during, and after four consecutive days of passive oral MPH treatment that was administered exclusively in the active phase (Fig. 4A). MPH consumption (mg/kg/day) data were analyzed by one-way ANOVA with group (F1 $Veh_{n=28}$, F1 $NIC_{n=24}$, or F2 $NIC_{n=31}$) as the sole factor, and, where appropriate, Bonferroni's multiple comparisons post-hoc test was applied. As shown in Fig. S2, there was a main effect of group on daily MPH consumption ($F_{2,80} = 3.28$; $p = 0.043$). Interestingly, F1 Veh mice consumed more MPH per day compared to F1 NIC and F2 NIC mice ($p = 0.049$ and $p = 0.046$, respectively).

For MPH-treated mice, home cage activity data were analyzed by three-way repeated measures ANOVA with the factors group (F1 $Veh_{n=28}$, F1 $NIC_{n=24}$, or F2 $NIC_{n=31}$), phase (active or inactive phase), and experimental stage (BL, MPH, or post-MPH). Where appropriate, Bonferroni's multiple comparisons post-hoc test was applied. Main effects of group ($F_{2,157} = 9.84$; $p = 0.00009$), phase ($F_{1,157} = 4.56$; $p = 0.036$), and experimental stage ($F_{2,314} = 24.18$; $p = 0.000005$) as

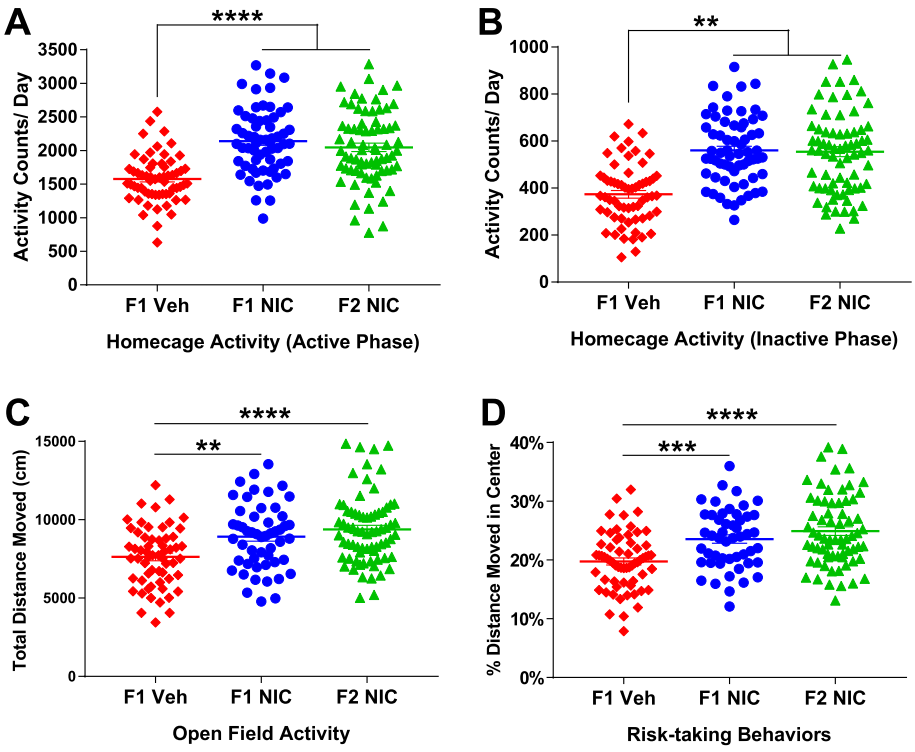

Fig. 2. *Adolescent DNE mice exhibit home cage hyperactivity during the active and inactive phases as well as hyperactivity and increased risk-taking in the open field.* Baseline (BL) data for home cage activity and open field behavior. **(A)** *Active phase home cage activity* (n_{F1Veh} = 61, n_{F1NIC} = 63, and n_{F2NIC} = 73). F1 NIC and F2 NIC mice were more active than F1 Veh during the active phase at baseline ($p = 1e^{-14}$ and $p = 2e^{-12}$, respectively). **(B)** *Inactive phase home cage activity* (n_{F1Veh} = 61, n_{F1NIC} = 63, and n_{F2NIC} = 73). F1 NIC and F2 NIC mice were more active than F1 Veh during the inactive phase at baseline ($p = 0.0091$ and $p = 0.0088$, respectively). **(C)** *Total distance moved (cm) in a 15-min open field (open field) trial* (n_{F1Veh} = 59, n_{F1NIC} = 63, and n_{F2NIC} = 71). F1 NIC and F2 NIC mice moved a greater total distance in the open field compared to F1 Veh ($p = 0.0039$ and $p = 0.00001$, respectively). **(D)** *Percent distance moved in the center of the open field* (n_{F1Veh} = 59, n_{F1NIC} = 63, and n_{F2NIC} = 71). F1 NIC and F2 NIC mice moved a greater percent of total distance in the center of the open field compared to Veh ($p = 0.0007$ and $p = 3.56e^{-7}$, respectively). All data are mean ± S.E.M. **p < 0.01; ***p < 0.001; ****p < 0.0001.

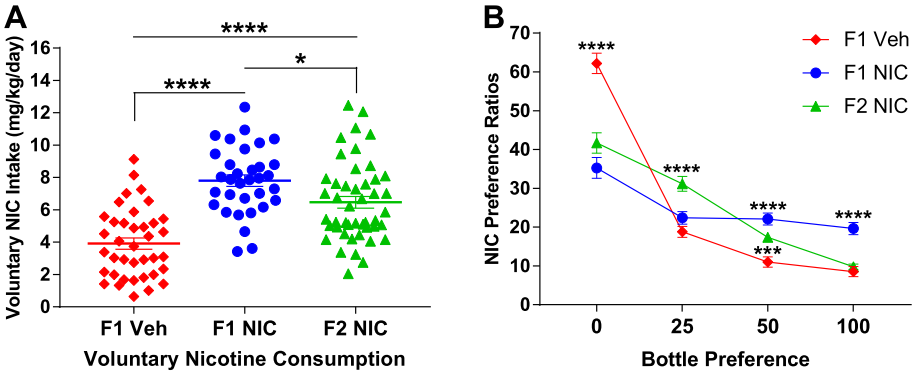

Fig. 3. *Adolescent DNE mice display increased voluntary nicotine intake and increased nicotine preference.* **(A)** *Voluntary nicotine intake (mg/kg/day) in the four-bottle choice test (FBCT)* (n_{F1Veh} = 38, n_{F1NIC} = 33, and n_{F2NIC} = 46). F1 NIC and F2 NIC mice consume more nicotine than F1 Veh ($p = 2.58e^{-10}$ and $p = 2.05e^{-5}$, respectively), and F1 NIC mice consume more nicotine than F2 NIC ($p = 0.031$). **(B)** *Nicotine preference ratios for the four-bottle choice test* (n_{F1Veh} = 38, n_{F1NIC} = 33, and n_{F2NIC} = 46). F2 NIC mice consume more 25μg/mL nicotine than F1 Veh and F1 NIC ($p = 3.59^{-6}$ and $p = 0.0014$, respectively). F1 NIC and F2 NIC mice consume more 50μg/mL nicotine than F1 Veh ($p = 0.00009$ and $p = 0.026$, respectively). F1 NIC mice consume more 100μg/mL nicotine than F1 Veh and F2 NIC ($p = 0.00007$ and $p = 0.00027$). F1 Veh mice consume more plain water (0μg/mL) than F1 NIC and F2 NIC mice ($p = 1.92e^{-15}$ and $p = 9.0e^{-14}$, respectively), and F2 NIC mice consume more plain water than F1 NIC ($p = 0.030$). All data are mean ± S.E.M. *p < 0.05; ***p < 0.001; ****p < 0.0001.

well as a significant group x experimental stage interaction ($F_{4,314} = 31.48$; $p = 3e^{-21}$), phase x experimental stage interaction ($F_{2,314} = 9.89$; $p = 0.00009$), and group x phase x experimental stage interaction ($F_{4,314} = 8.92$; $p = 0.000001$) were detected. F1 NIC and F2 NIC mice were less active in the active phase during MPH treatment compared to BL ($p = 1e^{-6}$ and $p = 2e^{-9}$), while F1 Veh mice were more active in the active phase during MPH treatment compared to BL ($p = 0.032$) and compared to F1 NIC and F2 NIC mice ($p = 0.015$ and $p = 0.002$, respectively) (Fig. 4B). The effects of MPH treatment were rapidly reversed, as F1 NIC and F2 NIC mice were more active in the active phase during the four days following cessation of MPH treatment (post-MPH) compared to F1 Veh ($p = 5e^{-6}$ and $p = 0.00008$, respectively). Results for inactive phase HC activity (Fig. 4C) were comparable to those for the active phase. F1 NIC and F2 NIC mice were less active in the inactive phase during MPH treatment compared to BL ($p = 2e^{-11}$ and $p = 3e^{-11}$, respectively), while F1 Veh mice were more active in the inactive phase during MPH treatment compared to BL ($p = 0.013$) and compared to DNE mice ($p = 0.0014$ and $p = 0.0081$, respectively). The effects of MPH treatment on inactive phase HC activity were also rapidly reversed, as F1 NIC and F2 NIC mice were more active in the inactive phase during post-MPH compared to F1 Veh ($p = 4e^{-7}$ and $p = 6e^{-6}$, respectively).

MPH treatment also affected activity (total distance moved) and risk-taking behaviors (percent distance moved in the center) in the open field. Total distance moved and percent distance moved in the center of the open field for MPH and post-MPH were analyzed by two-way repeated measures ANOVA with the factors group (F1 $Veh_{n=28}$, F1 $NIC_{n=24}$, or F2 $NIC_{n=31}$) and experimental stage (BL, MPH, or post-MPH). Where appropriate, Bonferroni's multiple comparisons post-hoc test was applied. A main effect of experimental stage ($F_{2,157} = 7.14$; $p = 0.001$) and a significant group x experimental stage interaction ($F_{4,157} = 10.84$; $p = 8e^{-8}$) were detected for total distance moved in the OF (Fig. 4D). There was no effect of MPH treatment on total distance moved in the OF for DNE mice, while F1 Veh mice moved a greater total distance in the OF immediately following MPH treatment compared to BL ($p = 8e^{-11}$) and compared to F1 NIC and F2 NIC mice ($p = 0.004$ and $p = 0.005$, respectively). There were no group differences in total distance moved in the OF following post-MPH. A main effect of experimental stage ($F_{2,157} = 5.08$; $p = 0.007$) and a significant group x experimental stage interaction ($F_{4,157} = 8.15$, $p = 5e^{-6}$) were

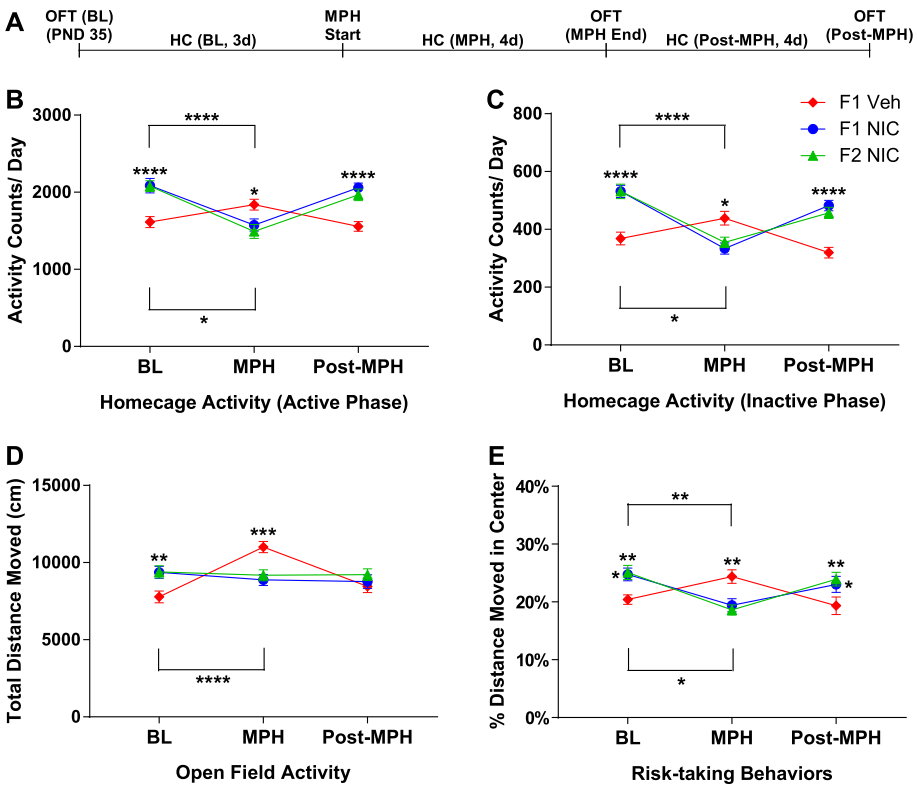

Fig. 4. *Passive oral MPH treatment normalizes home cage and open field activity and risk-taking behaviors in adolescent DNE mice.* **(A)** *Procedural timeline for MPH treatment and behavioral testing.* Home cage activity (n_{F1Veh} = 28, n_{F1NIC} = 24, and n_{F2NIC} = 31) was recorded for 3 days before (baseline, BL), 4 days during (MPH), and 4 days after (post-MPH) passive oral methylphenidate treatment. Open field behaviors (n_{F1Veh} = 28, n_{F1NIC} = 24, and n_{F2NIC} = 31) were tested before (baseline), immediately following (MPH), and 4d after (post-MPH) MPH treatment. **(B)** *Active phase HC activity*. F1 NIC and F2 NIC mice were less active in the active phase during MPH treatment compared to BL ($p = 1e^{-6}$ and $p = 2e^{-9}$) while F1 Veh mice were more active in the active phase during MPH treatment compared to BL ($p = 0.032$) and compared to F1 NIC and F2 NIC mice ($p = 0.015$ and $p = 0.002$, respectively). F1 NIC and F2 NIC mice were more active in the active phase during over four days following cessation of MPH treatment (post-MPH) compared to F1 Veh ($p = 5e^{-6}$ and $p = 0.00008$, respectively). **(C)** *Inactive phase HC activity*. F1 NIC and F2 NIC mice were less active in the inactive phase during MPH treatment compared to BL ($p = 2e^{-11}$ and $p = 3e^{-11}$, respectively), while F1 Veh mice were more active in the inactive phase during MPH treatment compared to BL ($p = 0.013$) and compared to DNE mice ($p = 0.0014$ and $p = 0.0081$, respectively). F1 NIC and F2 NIC mice were more active in the inactive phase during post-MPH compared to F1 Veh ($p = 4e^{-7}$ and $p = 6e^{-6}$, respectively). **(D)** *Total distance moved in the OF*. F1 Veh mice moved a greater total distance in the OF immediately following MPH treatment compared to BL ($p = 8e^{-11}$) and compared to F1 NIC and F2 NIC mice ($p = 0.004$ and $p = 0.005$, respectively). **(E)** *Percent distance moved in the center of the OF*. F1 NIC and F2 NIC mice moved a lesser percent distance in the center of the OF immediately following MPH treatment compared to BL ($p = 0.002$ and $p = 0.00003$, respectively), while F1 Veh mice moved a greater percent distance in the center of the OF immediately following MPH compared to BL ($p = 0.024$) and compared to F1 NIC and F2 NIC mice ($p = 0.004$ and $p = 0.0009$, respectively). F1 NIC and F2 NIC mice moved a greater percent distance in the center of the OF following post-MPH compared to F1 Veh ($p = 0.032$ and $p = 0.009$, respectively). All data are mean ± S.E.M. *$p < 0.05$; **$p < 0.01$; ***$p < 0.001$; ****$p < 0.0001$. Floating asterisks indicate between-group differences. Solid lines with asterisks indicate within-group differences for DNE mice (above) and F1 Veh mice (below).

detected for percent distance moved in the center of the OF (Fig. 4E). F1 NIC and F2 NIC mice moved a lesser percent distance in the center of the OF immediately following MPH treatment compared to BL ($p = 0.002$ and $p = 0.00003$, respectively), while F1 Veh mice moved a greater percent distance in the center of the OF immediately following MPH compared to BL ($p = 0.024$) and compared to F1 NIC and F2 NIC mice ($p = 0.004$ and $p = 0.0009$, respectively). F1 NIC and F2 NIC mice moved a greater percent distance in the center of the OF following post-MPH compared to F1 Veh ($p = 0.032$ and $p = 0.009$, respectively).

3.4. Effects of voluntary nicotine consumption in the four-bottle choice test on activity and risk-taking behaviors

The prevalent use of tobacco products by individuals with ADHD is thought to constitute self-medication (Amsterdam et al., 2018). Consequently, the impacts of voluntary nicotine consumption on home cage activity as well as activity and risk-taking behaviors in the open field were evaluated at baseline, in response to the four-bottle choice test, and over a 24 h nicotine withdrawal period (Fig. 5A). For four-bottle choice-tested mice, home cage activity data were analyzed by three-way repeated measures ANOVA with the factors group (F1 $Veh_{n=30}$, F1 $NIC_{n=32}$, or F2 $NIC_{n=33}$), phase (active or inactive phase), and experimental stage (BL, NIC1, NIC2, or WD). Where appropriate, Bonferroni's multiple comparisons post-hoc test was applied. Main effects of group ($F_{2,128} = 5.42$; $p = 0.006$), phase ($F_{1,363} = 5.55$; $p = 0.021$), and experimental stage ($F_{3,384} = 10.36$; $p = 0.000003$) as well as a significant group x experimental stage interaction ($F_{6,384} = 2.83$; $p = 0.13$), phase x experimental stage interaction ($F_{3,384} = 18.91$; $p = 8e^{-11}$), and group x phase x experimental stage interaction ($F_{3,384} = 4.95$; $p = 0.003$) were detected. For active phase home age activity (Fig. 5B) during the first four days of the FBCT (NIC 1) ($p = 0.00009$ and $p = 0.004$, respectively), second four days of the FBCT (NIC 2) ($p = 0.003$ and $p = 0.03$, respectively) and during withdrawal ($p = 1.12e^{-11}$ and $p = 1.2e^{-7}$, respectively), F1 NIC and F2 NIC mice were less active compared to BL but remained more active than F1 Veh ($p = 0.016$ and $p = 0.015$, respectively). In contrast, the FBCT had no effect on active phase HC activity in F1 Veh mice during NIC1 or WD, while activity was increased in F1 Veh mice during NIC2 compared to BL ($p = 0.002$). For inactive phase HC activity (Fig. 5C), F1 NIC and F2 NIC mice were less active in the inactive phase during NIC1 ($p = 6e^{-6}$ and $p = 3e^{-7}$, respectively), NIC2 ($p = 2e^{-6}$ and $p = 1e^{-6}$, respectively) and WD ($p = 2e^{-6}$ and $p = 0.0008$, respectively) compared to BL. In addition, F1 NIC and F2 NIC mice were more active than F1 Veh during WD ($p = 0.004$ and $p = 6e^{-7}$, respectively), and F1 Veh mice were less active during WD compared to BL ($p = 0.004$).

The four-bottle choice test also impacted activity and risk-taking behaviors in the open field. Total distance moved and percent distance moved in the center of the open field were analyzed by two-way repeated measures ANOVA with the factors group (F1 $Veh_{n=30}$, F1 $NIC_{n=24}$, or F2 $NIC_{n=35}$) and experimental stage (BL, NIC1, NIC2, or WD). Where appropriate, Bonferroni's multiple comparisons post-hoc test was applied. Main effects of group ($F_{2,90} = 19.05$; $p = 1e^{-7}$) and experimental stage ($F_{2,180} = 59.28$, $p = 1e^{-15}$) and a significant group x experimental stage interaction ($F_{4,180} = 2.70$; $p = 0.03$) were detected for total distance moved in the OF (Fig. 5D). F2 NIC mice moved a greater total distance in the OF compared to F1 NIC and F1 Veh mice immediately following the FBCT ($p = 1e^{-6}$ and $p = 0.0009$, respectively) and after a 24 h post-FBCT NIC WD period ($p = 0.00004$ and

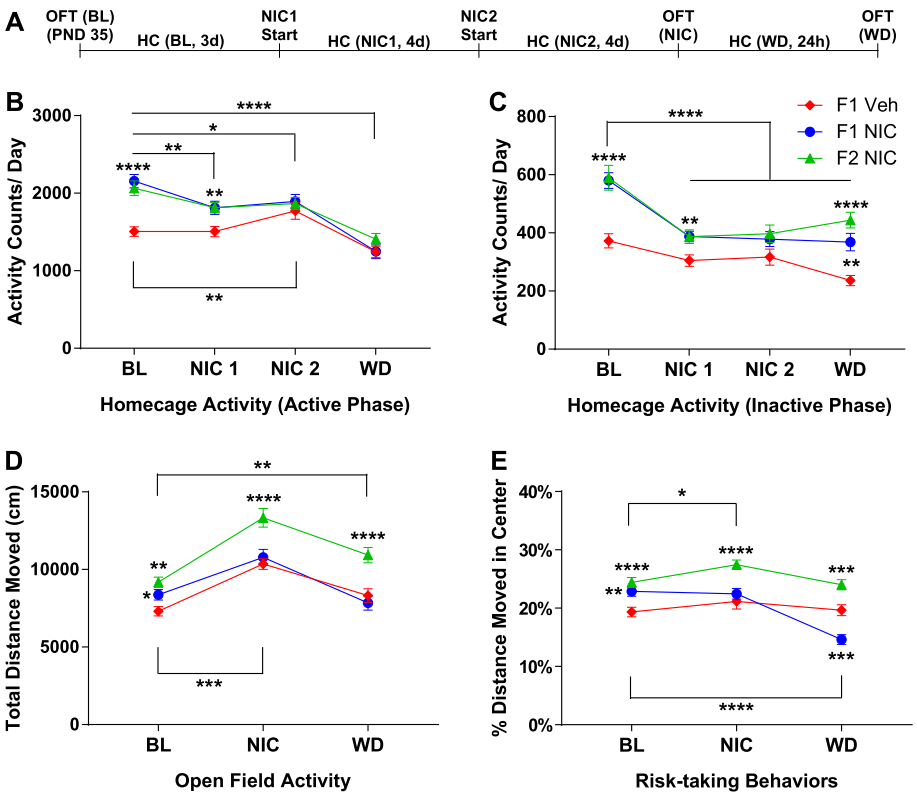

Fig. 5. *Adolescent DNE mice exhibit differential behavioral responses to voluntary nicotine intake and withdrawal.* **(A)** *Procedural timeline for nicotine administration in the four-bottle choice test and behavioral testing.* Home cage activity (n_{F1Veh} = 30, n_{F1NIC} = 32, and n_{F2NIC} = 33) was recorded over 3d before (baseline, BL), over two continuous 4d intervals during (NIC1 and NIC2), and over 24 h after (withdrawal, WD) voluntary nicotine intake in the four-bottle choice test (FBCT). Open field behavior (n_{F1Veh} = 30, n_{F1NIC} = 24, and n_{F2NIC} = 35) was tested before (BL), immediately following (nicotine, NIC), and 24 h after (WD) voluntary nicotine intake. **(B)** *Active phase HC activity*. F1 NIC and F2 NIC mice were more active than F1 Veh during NIC1 ($p = 0.016$ and $p = 0.015$, respectively) and were more active at BL compared to NIC1 ($p = 0.00009$ and $p = 0.004$, respectively), NIC2 ($p = 0.003$ and $p = 0.03$, respectively), and WD ($p = 1e^{-11}$ and $p = 1e^{-7}$, respectively). F1 Veh mice were more active during NIC2 compared to BL ($p = 0.002$). **(C)** *Inactive phase HC activity*. F1 NIC and F2 NIC mice were more active than F1 Veh during WD ($p = 0.004$ and $p = 6e^{-7}$, respectively) and were less active during NIC1 ($p = 6e^{-6}$ and $p = 3e^{-7}$, respectively), NIC2 ($p = 2e^{-6}$ and $1e^{-6}$, respectively) and WD ($p = 2e^{-6}$ and $p = 0.0008$, respectively) compared to BL. F1 Veh mice were less active during WD compared to BL ($p = 0.004$). **(D)** *Total distance moved (cm) in a 15-min open field (OF) trial.* F2 NIC mice moved a greater total distance in the OF compared to F1 NIC and F1 Veh mice immediately following the FBCT ($p = 0.000001$ and $p = 0.0009$, respectively) and after a 24 h post-FBCT NIC WD period ($p = 0.00004$ and $p = 0.00002$, respectively). F1 Veh, F1 NIC, and F2 NIC mice all moved a greater total distance in the OF immediately following voluntary NIC compared to BL ($p = 1e^{-6}$, $p = 0.0001$, and $p = 7e^{-16}$, respectively), but this effect persisted through 24 h NIC WD only in F2 NIC mice ($p = 0.0009$). **(E)** *Percent distance moved in the center of the OF*. F2 NIC mice moved a greater percent distance in the center of the OF immediately following the FBCT compared to BL ($p = 0.005$) and after 24 h NIC WD compared to F1 Veh and F1 NIC ($p = 0.0006$ and $p = 3e^{-6}$, respectively). F1 NIC mice moved a lesser percent distance in the center of the OF after 24 h NIC WD compared to BL ($p = 7e^{-8}$) and compared to F1 Veh and F2 NIC ($p = 0.002$ and $p = 3e^{-6}$, respectively). All data are mean ± S.E.M. *$p < 0.05$; **$p < 0.01$; ***$p < 0.001$; ****$p < 0.0001$. Floating asterisks indicate between-group differences. For panels B–D, solid lines with asterisks indicate within-group differences for DNE mice (above) and F1 Veh mice (below). For panel E, solid lines with asterisks indicate within-group differences for F2 NIC mice (above) and F1 NIC mice (below).

p = 0.00002, respectively). F1 Veh, F1 NIC, and F2 NIC mice all moved a greater total distance in the OF immediately following voluntary NIC compared to BL ($p = 1e^{-6}$, $p = 0.0001$, and $p = 7e^{-16}$, respectively), but this effect persisted through 24 h NIC WD only in F2 NIC mice ($p = 0.0009$). Main effects of group ($F_{2,90} = 25.34$; $p = 2e^{-8}$) and experimental stage ($F_{2,180} = 19.47$; $p = 2e^{-7}$) and a significant group x experimental stage interaction ($F_{4,180} = 7.53$; $p = 0.00001$) were also detected for percent distance moved in the center of the OF (Fig. 5E). F2 NIC mice moved a greater percent distance in the center of the OF immediately following the FBCT compared to BL ($p = 0.005$) and after 24 h NIC WD compared to F1 Veh and F1 NIC ($p = 0.0006$ and $p = 3e^{-6}$, respectively). F1 NIC mice moved a lesser percent distance in the center of the OF after 24 h NIC WD compared to BL ($p = 7e^{-8}$) and compared to F1 Veh and F2 NIC ($p = 0.002$ and $p = 3e^{-6}$, respectively).

3.5. Rhythmometric analyses of home cage activity in DNE mice at baseline and in response to MPH and nicotine

ADHD patients exhibit a discrete profile of circadian anomalies including increased MESOR and amplitude and phase-delay of rest-wake activity rhythms (Baird et al., 2012; Van Veen et al., 2010; Imeraj et al., 2012; Bijlenga et al., 2013; Snitselaar et al., 2017), each of which exhibit MPH-responsiveness and are positively correlated with nicotine use (Snitselaar et al., 2017; Wittmann et al., 2006). To further evaluate the construct validity of our ADHD model, rhythmometric analyses were performed to evaluate potential DNE-induced ADHD-like perturbations in the rhythmicity of home cage activity and responsiveness to MPH treatment and nicotine consumption. Analyses revealed near-24 h fundamental periods (circadian rhythms) of home cage activity accompanied by multiple underlying harmonics of shorter periods (ultradian rhythms) (data not shown, but are available upon request). There were no significant within-group or between-group differences in the duration of the fundamental period at baseline or during MPH or four-bottle choice test testing (data not shown, but are available upon request). Given the absence of prior research exploring differences in the ultradian rhythmicity of activity in ADHD patients, we elected to focus this report on global parameter estimates which describe the composite home cage activity rhythms, namely the MESOR (midline of rhythm), global amplitude (0.5× peak – trough), and orthophase (latency to peak), since these parameters are the most comparable to available measures of activity rhythms in humans. A detailed description of rhythmometric procedures and a schematic depicting the global parameters used to characterize home cage activity rhythms are provided in the supplement (Fig. S3). Representative curve fits for each experimental stage of home cage activity monitoring are provided in the supplement (Fig. S4).

We first compared global measures of rhythmicity at baseline to elucidate potential ADHD-like changes in the home cage activity rhythms of DNE mice. Baseline rhythmometric datasets (MESOR, global amplitude, and orthophase) were analyzed by one-way ANOVA with group (F1 $Veh_{n=61}$, F1 $NIC_{n=63}$, or F2 $NIC_{n=73}$) as the sole factor, and, where appropriate, Bonferroni's multiple comparisons post-hoc test was applied. There was a main effect of group ($F_{2,193} = 27.07$; $p = 4e^{-11}$) on MESOR estimates at baseline (Fig. 6A). F1 NIC and F2 NIC mice had increased MESOR estimates at baseline compared to F1 Veh

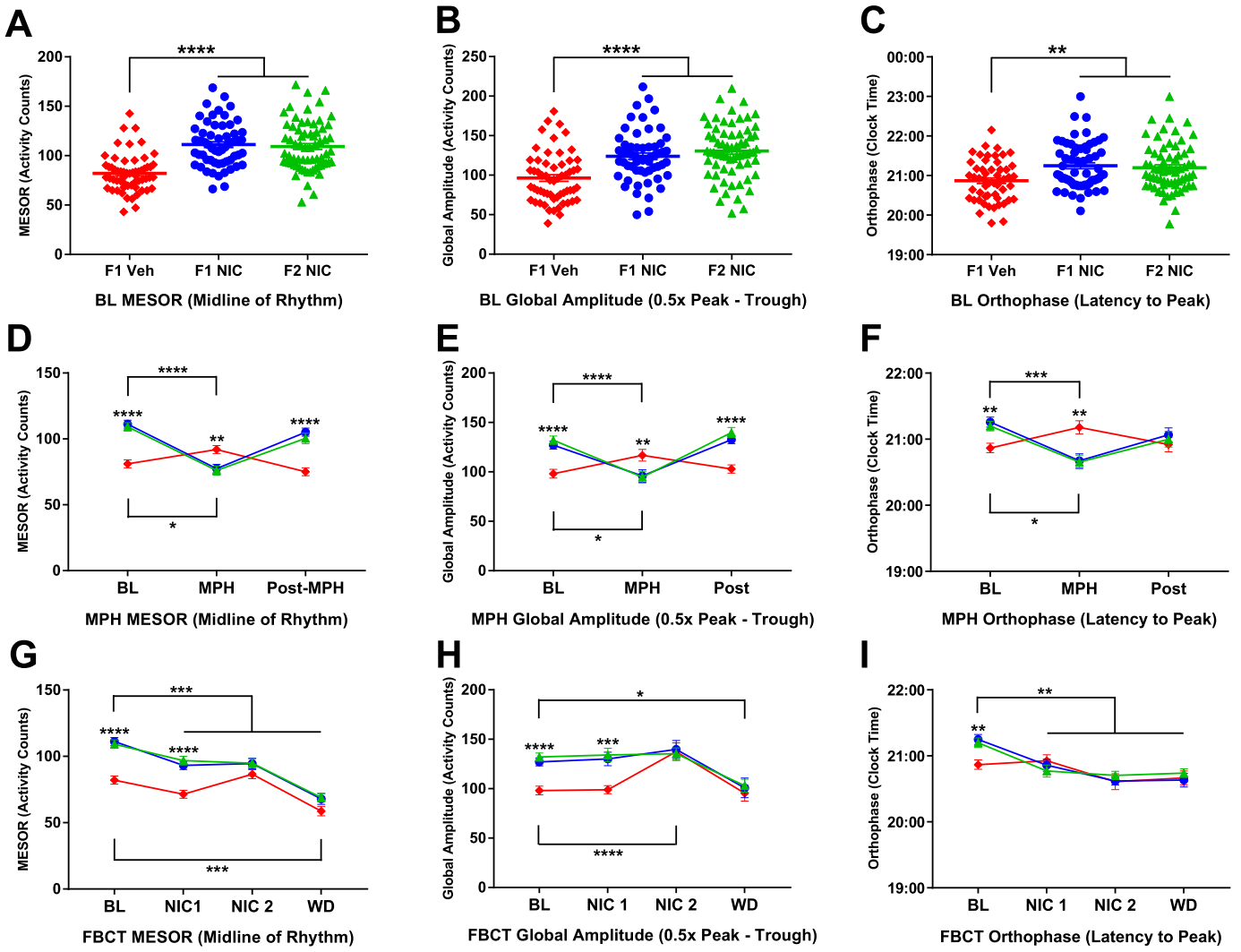

Fig. 6. *Adolescent DNE mice show ADHD-like deficits in rhythmicity of activity that are normalized by methylphenidate and partially normalized by nicotine.* **(A–C)** MESOR, global amplitude, and orthophase of home cage activity rhythms at baseline (n_{F1Veh} = 61, n_{F1NIC} = 63, and n_{F2NIC} = 73), **(D–F)** MESOR, global amplitude, and orthophase estimates for mice that underwent **(J–L)** passive oral MPH treatment (n_{F1Veh} = 28, n_{F1NIC} = 24, and n_{F2NIC} = 31), and **(G–I)** four-bottle choice test testing (n_{F1Veh} = 30, n_{F1NIC} = 32, and n_{F2NIC} = 33). **(A)** *MESOR estimates at BL.* F1 NIC and F2 NIC mice had increased MESOR estimates at BL compared to F1 Veh ($p = 5e^{-10}$ and $p = 2e^{-8}$, respectively). **(B)** *Global amplitude estimates at BL.* F1 NIC and F2 NIC mice had increased global amplitude estimates at BL compared to F1 Veh mice (p = 0.00003 and $5e^{-8}$, respectively). **(C)** *Orthophase estimates at BL.* F1 NIC and F2 NIC mice had delayed orthophase estimates at BL compared to F1 Veh (p = 0.0003 and p = 0.006, respectively). **(D)** *MESOR estimates for MPH treatment.* F1 NIC and F2 NIC mice had decreased MESOR values during MPH treatment compared to BL ($p = 3e^{-11}$ and $p = 1e^{-12}$, respectively). F1 Veh mice had increased MESOR estimates during MPH compared to BL (p = 0.033) and compared to F1 NIC and F2 NIC (p = 0.005 and p = 0.003, respectively). F1 NIC and F2 NIC mice had increased MESOR estimates compared to F1 Veh during post-MPH ($p = 5e^{-8}$ and $p = 7e^{-7}$, respectively). **(E)** *Global amplitude estimates for MPH treatment.* F1 NIC and F2 NIC mice had decreased global amplitude estimates during MPH compared to BL (p = 0.00009 and $p = 1e^{-7}$). F1 Veh mice had increased global amplitude estimates during MPH compared to BL (p = 0.042) and compared to F1 NIC and F2 NIC (p = 0.002 and p = 0.004, respectively). F1 NIC and F2 NIC mice had increased global amplitude estimates compared to F1 Veh during post-MPH (p = 0.0004 and p = 0.00003, respectively). **(F)** *Orthophase estimates for MPH treatment.* F1 NIC and F2 NIC mice had advanced orthophase estimates during MPH compared to BL (p = 0.009 and p = 0.0007, respectively). F1 Veh mice had delayed orthophase estimates during MPH compared to BL (p = 0.046) and compared to F1 NIC and F2 NIC (p = 0.008 and p = 0.003, respectively). There were no group differences in orthophase estimates during post-MPH. **(G)** *MESOR estimates for the FBCT.* F1 NIC and F2 NIC mice decreased MESOR estimates compared to BL during NIC1 (p = 0.0001 and p = 0.0008, respectively), NIC2 (p = 0.0002 and p = 0.0003, respectively), and WD ($p = 1e^{-16}$ and $p = 1e^{-15}$, respectively). F1 NIC and F2 NIC mice had increased MESOR estimates compared to F1 Veh during NIC1 (p = 0.0003 and p = 0.000002, respectively) but not NIC2 or WD. F1 Veh mice had decreased MESOR estimates during WD compared to BL (p = 0.0005). **(H)** *Global amplitude estimates for the FBCT.* F1 NIC and F2 NIC mice had decreased global amplitude estimates during WD compared to BL (p = 0.02 and p = 0.01, respectively) and had increased global amplitude estimates compared to F1 Veh during NIC1 (p = 0.0004 and p = 0.00002) but not NIC2 or WD. F1 Veh mice had increased global amplitude estimates during NIC2 compared to BL (p = 0.00008). **(I)** *Orthophase estimates for the FBCT.* F1 NIC and F2 NIC mice had advanced orthophase estimates for NIC1 (p = 0.007 and p = 0.002, respectively), NIC2 (p = 0.0001 and p = 0.0003, respectively), and WD (p = 0.006 and p = 0.009, respectively) compared to BL, while F1 Veh mice did not differ from BL at any stage of FBCT testing. *p < 0.05; **p < 0.01; ***p < 0.001; ****p < 0.0001. For panels D–I, floating asterisks indicate between-group differences, while solid lines with asterisks indicate within-group differences for DNE mice (above) and F1 Veh mice (below). MESOR: midline estimating statistic of rhythm (measure of central tendency); global amplitude: difference between peak and trough (measure of the magnitude of change over a given cycle); orthophase: clock time at peak (maximum value) of activity counts (measure of latency to peak activity).

($p = 5.4e^{-10}$ and $p = 2.3e^{-8}$, respectively). Similarly, there was a main effect of group ($F_{2,193} = 18.87$; $p = 4e^{-8}$) on global amplitude estimates at baseline (Fig. 6B). F1 NIC and F2 NIC mice had increased global amplitude estimates at baseline compared to F1 Veh mice ($p = 0.00003$ and $6e^{-8}$, respectively). There was also a main effect of group ($F_{2,193} = 7.31$; $p = 0.0009$) on orthophase estimates at baseline (Fig. 6C). F1 NIC and F2 NIC mice had delayed orthophase estimates (increased latency to peak activity) at baseline compared to F1 Veh ($p = 0.0003$ and $p = 0.006$, respectively).

Considering that MPH exerts a normalizing effect on circadian rest-wake activity rhythms in ADHD patients (Snitselaar et al., 2017), the effects of MPH on the rhythmicity of home cage activity were evaluated to assess the treatment responsivity of ADHD-like rhythmometric anomalies in DNE mice. MESOR, global amplitude, and orthophase estimates for MPH-treated mice were analyzed by two-way repeated measures ANOVA with the factors group (F1 $Veh_{n=28}$, F1 $NIC_{n=24}$, or F2 $NIC_{n=31}$) and experimental stage (BL, MPH, or post-MPH). Where appropriate, Bonferroni's multiple comparisons post-hoc test was applied. Main effects of group ($F_{2,80} = 8.45$; $p = 0.0004$) and experimental stage ($F_{2,160} = 33.07$; $p = 9e^{-13}$) and a significant group x experimental stage interaction ($F_{4,160} = 17.81$; $p = 4e^{-12}$) were detected for MESOR in MPH-treated mice (Fig. 6D). F1 NIC and F2 NIC mice had decreased MESOR values during MPH compared to BL ($p = 3e^{-11}$ and $p = 1e^{-12}$, respectively). In contrast, F1 Veh mice had increased MESOR estimates during MPH compared to BL ($p = 0.033$) and compared to F1 NIC and F2 NIC ($p = 0.005$ and $p = 0.003$, respectively). F1 NIC and F2 NIC mice had increased MESOR estimates compared to F1 Veh during post-MPH ($p = 5e^{-8}$ and $p = 7e^{-7}$, respectively). MPH treatment also affected global amplitude. Main effects of MPH treatment were detected for both group ($F_{2,80} = 5.38$; $p = 0.006$) and experimental stage ($F_{2,160} = 22.15$; $p = 3e^{-9}$), and there was a significant group x experimental stage interaction ($F_{4,160} = 8.87$; $p = 2e^{-6}$) (Fig. 6E). F1 NIC and F2 NIC mice had decreased global amplitude estimates during MPH compared to BL ($p = 0.00009$ and $p = 1e^{-7}$). F1 Veh mice had increased global amplitude estimates during MPH compared to BL ($p = 0.042$) and compared to F1 NIC and F2 NIC ($p = 0.002$ and $p = 0.004$, respectively). During post-MPH, F1 NIC and F2 NIC mice had increased global amplitude estimates compared to F1 Veh ($p = 0.0004$ and $p = 0.00003$, respectively). A main effect of experimental stage ($F_{2,160} = 3.68$; $p = 0.027$) and a significant group x experimental stage interaction ($F_{4,160} = 5.08$; $p = 0.007$) were detected for orthophase in MPH-treated mice (Fig. 6F). F1 NIC and F2 NIC mice had advanced orthophase estimates during MPH compared to BL ($p = 0.009$ and $p = 0.0007$, respectively). Conversely, F1 Veh mice had delayed orthophase estimates during MPH compared to BL ($p = 0.046$) and compared to F1 NIC and F2 NIC ($p = 0.008$ and $p = 0.003$, respectively). There were no group differences in orthophase estimates during post-MPH.

Nicotine use is positively correlated with the magnitude of circadian anomalies in ADHD (Wittmann et al., 2006) and ADHD patients report exaggerated withdrawal symptoms (Gray et al., 2010; Bidwell et al., 2018). Thus, we evaluated the effects of voluntary nicotine consumption and withdrawal on the rhythmicity of home cage activity in DNE mice. MESOR, global amplitude, and orthophase estimates for four-bottle choice-tested mice were analyzed by two-way repeated measures ANOVA with the factors group (F1 $Veh_{n=30}$, F1 $NIC_{n=32}$, or F2 $NIC_{n=33}$) and experimental stage (BL, NIC1, NIC2, or WD). Where appropriate, Bonferroni's multiple comparisons post-hoc test was applied. Main effects of group ($F_{2,100} = 24.03$; $p = 3e^{-9}$) and experimental stage ($F_{3,300} = 27.47$; $p = 1e^{-15}$) and a significant group x experimental stage interaction ($F_{6,300} = 4.83$; $p = 0.0001$) were detected for MESOR in FBCT-tested mice (Fig. 6G). F1 NIC and F2 NIC mice had decreased MESOR estimates compared to BL during NIC1 ($p = 0.0001$ and $p = 0.0008$, respectively), NIC2 ($p = 0.0002$ and $p = 0.0003$, respectively), and WD ($p = 1e^{-16}$ and $p = 1e^{-15}$, respectively). F1 NIC and F2 NIC mice also had increased MESOR estimates compared to F1 Veh during NIC1 ($p = 0.0003$ and $p = 0.000002$, respectively) but not NIC2 or WD. F1 Veh mice had decreased MESOR estimates during WD compared to BL ($p = 0.0005$). The FBCT also impacted global amplitude. Main effects of group ($F_{2,100} = 10.11$; $p = 0.0001$) and experimental stage ($F_{3,300} = 11.44$; $p = 4e^{-7}$) and a significant group x experimental stage interaction ($F_{6,300} = 3.83$; $p = 0.001$) were detected (Fig. 6H). F1 NIC and F2 NIC mice had decreased global amplitude estimates during WD compared to BL ($p = 0.02$ and $p = 0.01$, respectively) and had increased global amplitude estimates compared to F1 Veh during NIC1 ($p = 0.0004$ and $p = 0.00002$) but not NIC2 or WD. F1 Veh mice had increased global amplitude estimates during NIC2 compared to BL ($p = 0.00008$). A main effect of experimental stage ($F_{3,300} = 7.79$; $p = 0.00005$) and a significant group x experimental stage interaction ($F_{6,300} = 2.25$; $p = 0.04$) were detected for orthophase in FBCT-tested mice (Fig. 6I). F1 NIC and F2 NIC mice had advanced orthophase estimates for NIC1 ($p = 0.007$ and $p = 0.002$, respectively), NIC2 ($p = 0.0001$ and $p = 0.0003$, respectively), and WD ($p = 0.006$ and $p = 0.009$, respectively) compared to BL, while F1 Veh mice did not differ from baseline at any stage of FBCT testing.

It should be noted that neither MPH or nicotine intake covaried with any of the behaviors assessed (Table S2), indicating that the observed within- and between-group behavioral differences in drug responsivity are not driven by variations in drug intake.

3.6. Impacts of DNE on nAChR binding and nicotine-induced DA release in striatum

The impacts of DNE on striatal nAChR expression were evaluated by assaying subtype-selective nAChR binding. Data for striatal nAChR binding were analyzed by one-way ANOVA with group (F1 $Veh_{n=12}$, F1 $NIC_{n=13}$, or F2 $NIC_{n=13}$) as the sole factor, and, where appropriate, Holm-Sidak's multiple comparisons post-hoc test was applied. A main effect of group was detected for cytisine-resistant (non-α4β2* nAChR) [^{125}I]-epibatidine binding in striatum ($F_{2,\ 34} = 3.29$; $p = 0.049$). F2 NIC mice had increased cytisine-resistant [^{125}I]-epibatidine binding in striatum compared to F1 Veh ($p = 0.047$) (Fig. 7A, left). There was no main effect of group on cytisine-sensitive (α4β2* nAChR) [^{125}I]-epibatidine binding in striatum (Fig. 7A, right). Similarly, there was no main effect of group on α-conotoxinMII-resistant (non-α6β2* nAChR) [^{125}I]-epibatidine binding in striatum (Fig. 7B, left). A main effect of group was detected for α-conotoxinMII-sensitive (α6β2* nAChR) [^{125}I]-epibatidine binding in striatum ($F_{2,33} = 5.095$; $p = 0.012$). F1 NIC mice had decreased α-conotoxinMII-sensitive [^{125}I]-epibatidine binding compared to F1 Veh and F2 NIC ($p = 0.026$ and $p = 0.008$, respectively) (Fig. 7B, right).

The effects of DNE on subtype-selective nAChR-mediated nicotine-induced striatal DA release were characterized by assaying α-CtxMII-resistant (non-α6β2* nAChR-mediated) and α-CtxMII-sensitive (α6β2* nAChR-mediated) nicotine-induced DA release in striatum. Data for nAChR-mediated DA release were analyzed by one-way ANOVA with group (F1 $Veh_{n=18}$, F1 $NIC_{n=21}$, or F2 $NIC_{n=14}$) as the sole factor, and, where appropriate, Holm-Sidak's multiple comparisons post-hoc test was applied. ANOVA revealed main effects of group for maximal nicotine-induced DA release (R_{max}) and nicotine EC_{50} ($F_{2,50} = 11.4$; $p = 0.00008$ and $F_{2,50} = 6.47$; $p = 0.003$, respectively) for the α-CtxMII-resistant fraction. F1 NIC and F2 NIC mice had increased α-CtxMII-resistant DA R_{max} ($p = 0.00006$ and $p = 0.008$, respectively) (Fig. 7C, left) and decreased nicotine EC_{50} ($p = 0.029$ and $p = 0.002$, respectively) estimates compared to F1 Veh (Fig. 7C, right). There was also a main effect of group on α-CtxMII-sensitive striatal nicotine-induced DA R_{max} ($F_{2,50} = 6.45$; $p = 0.003$). Similar to results for the α-CtxMII-resistant component, F1 NIC and F2 NIC mice had increased DA R_{max} ($p = 0.00001$ and $p = 0.006$, respectively) estimates compared to F1 Veh (Fig. 7D, left). F2 NIC mice had increased nicotine EC_{50} estimates compared to F1 Veh ($p = 0.038$) for α-CtxMII-sensitive nicotine-induced striatal DA release (Fig. 7D, right). Concentration-response

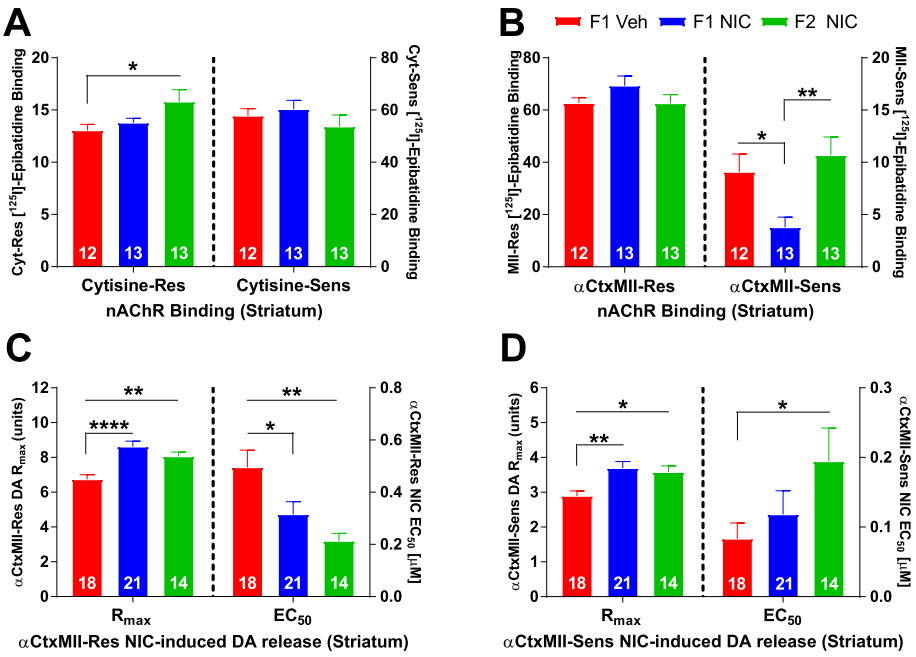

Fig. 7. *Adolescent DNE mice have altered nAChR binding and nicotine-induced DA release in striatum.* Nicotinic acetylcholine receptor (nAChR) binding (top) and nicotine-induced DA release (bottom). **(A)** *(Left) Cytisine-resistant (non-α4β2* nAChR) and (Right) cytisine-sensitive (α4β2* nAChR) [^{125}I]-epibatidine binding in striatum* (n_{F1Veh} = 12, n_{F1NIC} = 13, and n_{F2NIC} = 13). F2 NIC mice had increased cytisine-resistant [^{125}I]-epibatidine binding in striatum compared to F1 Veh (p = 0.047). **(B)** *(Left) α-conotoxinMII-resistant (non-α6β2* nAChR) and (Right) α-conotoxinMII-sensitive (α6β2* nAChR) [^{125}I]-epibatidine binding in striatum* (n_{F1Veh} = 12, n_{F1NIC} = 13, and n_{F2NIC} = 13). F1 NIC mice had decreased α-conotoxinMII-sensitive [^{125}I]-epibatidine binding in striatum compared to F1 Veh (p = 0.026) and F2 NIC (p = 0.008). **(C)** *(Left) nicotine-induced DA R_{max} (maximal nicotine-induced DA release) and (Right) nicotine EC_{50} (nicotine concentration eliciting half-maximal DA release) for α-conotoxinMII-resistant nicotine-induced striatal DA release* (n_{F1Veh} = 18, n_{F1NIC} = 21, and n_{F2NIC} = 14). F1 NIC and F2 NIC mice had increased α-conotoxinMII-resistant increased DA R_{max} (p = 0.000061 and p = 0.0087, respectively) and decreased nicotine EC_{50} (p = 0.029 and p = 0.0022, respectively) estimates compared to F1 Veh for α-conotoxinMII-resistant nicotine-induced striatal DA release. **(D)** *(Left) nicotine-induced DA R_{max} and (Right) nicotine EC_{50} for α-conotoxinMII-sensitive nicotine-induced striatal DA release* (n_{F1Veh} = 18, n_{F1NIC} = 21, and n_{F2NIC} = 14). F1 NIC and F2 NIC mice had increased DA R_{max} (p = 0.00001 and p = 0.0066, respectively) estimates compared to F1 Veh for α-conotoxinMII-sensitive nicotine-induced striatal DA release, and F2 NIC mice had increased nicotine EC_{50} estimates compared to F1 Veh (p = 0.038). All data are mean ± S.E.M. *p < 0.05; **p < 0.01; ***p < 0.0001; ****p < 0.0001.

curves used to derive R_{max} and EC_{50} estimates are provided in the supplement (Fig. S5).

3.7. Effects of DNE on nAChR binding and function in frontal cortex

The impacts of DNE on nAChR expression and function in frontal cortex were evaluated by assaying subtype-selective nAChR binding and ACh-evoked $^{86}Rb^+$ efflux for components with high and low sensitivity to ACh stimulation. Datasets for nAChR binding and nAChR-mediated $^{86}Rb^+$ efflux were analyzed by one-way ANOVA with group (F1 $Veh_{n=12}$, F1 $NIC_{n=12}$, or F2 $NIC_{n=11}$) as the sole factor, and, where appropriate, Holm-Sidak's multiple comparisons post-hoc test was applied. A main effect of group was detected for cytisine-resistant (non-α4β2* nAChR) [^{125}I]-epibatidine binding in frontal cortex ($F_{2,26}$ = 3.57; p = 0.043). F2 NIC mice had decreased cytisine-resistant [^{125}I]-epibatidine binding in frontal cortex compared to F1 Veh (p = 0.027) (Fig. 8A, left). In addition, the Kruskal-Wallis test detected a significant median difference among groups (H = 7.23; p = 0.027) for cytisine-sensitive (α4β2* nAChR) [^{125}I]-epibatidine binding in frontal cortex. F2 NIC mice had decreased mean rank cytisine-sensitive [^{125}I]-epibatidine binding in frontal cortex compared to F1 Veh (p = 0.025) (Fig. 8A, right). There was no main effect of group on high ACh sensitivity cortical $^{86}Rb^+$ efflux R_{max} (Fig. 8B, left), but a main effect of group ($F_{2,32}$ = 16.36; p = 0.00001) was detected for low ACh sensitivity cortical $^{86}Rb^+$ efflux R_{max} (Fig. 8B, right). F1 NIC and F2 NIC mice had decreased low ACh sensitivity $^{86}Rb^+$ efflux R_{max} estimates compared to F1 Veh (p = 0.002 and p = 0.0001, respectively). Main effects of group on ACh EC_{50} estimates were detected for both high (Fig. 8C, left) and low (Fig. 8C, right) ACh sensitivity cortical $^{86}Rb^+$ efflux ($F_{2,32}$ = 36.15; p = 4.85^{e-9} and $F_{2,32}$ = 15.87; p = 0.00001, respectively). F2 NIC mice had increased ACh EC_{50} estimates for the high ACh sensitivity component compared to F1 Veh and F1 NIC (p = $6.43e^{-7}$ and p = $9.69e^{-9}$, respectively), while F1 Veh mice had increased ACh EC_{50} estimates for the low ACh sensitivity component compared to both F1 NIC and F2 NIC (p = 0.0001 and p = 0.00006, respectively). A main effect of group ($F_{2,32}$ = 39.4; p = $2.34e^{-9}$) was detected for ratios of high versus low ACh sensitivity cortical $^{86}Rb^+$ efflux R_{max} (Fig. 8D). F1 NIC and F2 NIC mice had increased ratios of high versus low ACh sensitivity R_{max} fractions compared to F1 Veh (p = 0.004 and p = $1.32e^{-9}$, respectively), and F2 NIC mice had increased ratios of high versus low ACh sensitivity R_{max} fractions compared to F1 NIC (p = 0.00002). Concentration-response curves used to derive R_{max} and EC_{50} estimates are provided in the supplement (Fig. S5).

3.8. Impacts of DNE on dopamine transporter (DAT) function in striatum and frontal cortex

The effects of DNE on DAT-mediated DA uptake in striatum and frontal cortex were assessed by measuring DAT-specific [^{3}H]-DA uptake at two concentrations of [^{3}H]-DA, 0.05 μM (low concentration, approximate K_m for DAT-mediated maximal DA uptake) and 1.0 μM (high concentration, approximately 20× K_m for DAT-mediated maximal DA uptake). Data for DAT-mediated DA uptake were analyzed by one-way ANOVA with group (F1 $Veh_{n(FCX)=4\ n(STR)=4}$, F1 $NIC_{n(FCX)=9;\ n(STR)=8}$, or F2 $NIC_{n(FCX)=8;\ n(STR)=7}$) as the sole factor, and, where appropriate, Holm-Sidak's multiple comparisons post-hoc test was applied. Main effects of group were detected for [^{3}H]-DA uptake at both 0.05 μM [^{3}H]-DA (Fig. 9A, left) and 1.0 μM [^{3}H]-DA (Fig. 9A, right) in striatum ($F_{2,15}$ = 7.75; p = 0.005 and $F_{2,15}$ = 17.42; p = 0.0001, respectively). F1 NIC and F2 NIC mice had decreased [^{3}H]-DA uptake compared to F1 Veh at both 0.05 μM [^{3}H]-DA (p = 0.0038 and p = 0.0083, respectively) and 1.0 μM [^{3}H]-DA (p = 0.0002 and p = 0.0001, respectively). In frontal cortex, there was also a main effect of group ($F_{2,17}$ = 6.67; p = 0.007) on [^{3}H]-DA uptake at 0.05 μM [^{3}H]-DA (Fig. 9B, left). F1 NIC and F2 NIC mice exhibited reduced [^{3}H]-DA uptake compared to F1 Veh (p = 0.004 and p = 0.029, respectively). There was no main effect of group on [^{3}H] DA uptake at 1.0 μM [^{3}H]-DA (Fig. 9B, right) in frontal cortex. Lastly, the ratios of 1.0 μM [^{3}H]-DA uptake vs. 0.05 μM [^{3}H]-DA uptake were calculated for both striatum (Fig. 9C, left) and frontal cortex (Fig. 9C, right) to provide crude estimates of potential changes in DAT K_m (Grady et al., 2007). A main effect of group was detected for the DA uptake ratio in frontal cortex ($F_{2,17}$ = 27.15; p = $5.1e^{-6}$). F1 NIC mice had a greater [^{3}H]-DA uptake ratio in frontal

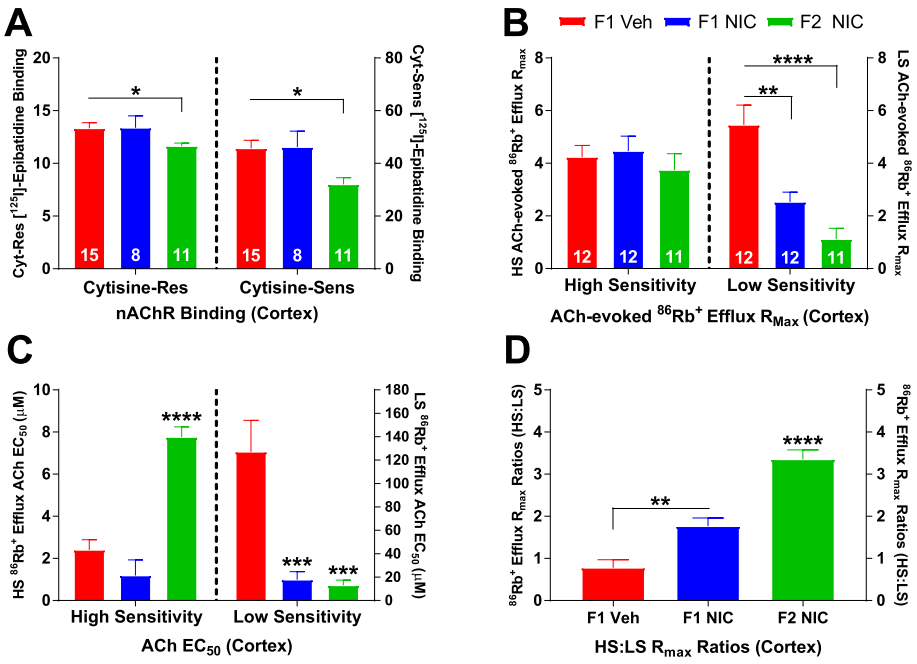

Fig. 8. *Adolescent DNE mice show altered nAChR binding and function in frontal cortex.* Nicotinic acetylcholine receptor (nAChR) binding and function in frontal cortex. **(A)** *(Left) cytisine-resistant and (Right) cytisine-sensitive [^{125}I]-epibatidine binding in frontal cortex* (n_{F1Veh} = 12, n_{F1NIC} = 12, and n_{F2NIC} = 11). F2 NIC mice had decreased cytisine-resistant [^{125}I]-epibatidine binding in frontal cortex compared to F1 Veh (p = 0.027). In addition, F2 NIC mice had decreased mean rank cytisine-sensitive [^{125}I]-epibatidine binding in frontal cortex compared to F1 Veh (p = 0.025). **(B)** *(Left) High ACh sensitivity and (Right) low ACh sensitivity $^{86}Rb^+$ efflux R_{max} in frontal cortex* (n_{F1Veh} = 12, n_{F1NIC} = 12, and n_{F2NIC} = 11). F1 NIC and F2 NIC mice had decreased low ACh sensitivity $^{86}Rb^+$ efflux R_{max} estimates compared to F1 Veh (p = 0.002 and p = 0.0001, respectively). **(C)** *(Left) High ACh sensitivity and (Right) low ACh sensitivity ACh EC_{50} in frontal cortex* (n_{F1Veh} = 12, n_{F1NIC} = 12, and n_{F2NIC} = 11). F2 NIC mice had increased ACh EC_{50} estimates for high ACh sensitivity cortical $^{86}Rb^+$ efflux compared to F1 Veh and F1 (p = 6.43e^{-7} and p = 9.69e^{-9}, respectively), while F1 Veh mice had increased ACh EC_{50} estimates for low ACh sensitivity cortical $^{86}Rb^+$ efflux compared to both F1 NIC and F2 NIC (p = 0.0001 and p = 0.00006, respectively). **(D)** *Ratios of high ACh sensitivity versus low ACh sensitivity $^{86}Rb^+$ efflux R_{max}* (n_{F1Veh} = 12, n_{F1NIC} = 12, and n_{F2NIC} = 11). F1 NIC and F2 NIC mice had increased ratios of high versus low ACh sensitivity cortical $^{86}Rb^+$ efflux R_{max} estimates compared to F1 Veh (p = 0.004 and p = 1.32e^{-9}, respectively), and F2 NIC mice had increased ratios of high versus low ACh sensitivity cortical $^{86}Rb^+$ efflux R_{max} estimates compared to F1 NIC (p = 0.00002). All data are mean ± S.E.M. *p < 0.05; **p < 0.01; ***p < 0.0001; ****p < 0.0001.

cortex compared to F1 Veh (p = 0.00005) and F2 NIC (p = 0.00002) mice, indicating a potential shift in K_m for F1 NIC mice. There was no main effect of group on the ratio of [^{3}H]-DA uptake in striatum.

3.9. Effects of DNE on the global DNA methylome in striatum and frontal cortex

Studies have shown that nicotine exposure alters DNA methylation. Therefore, the impact of DNE on global DNA methylation in striatum and frontal cortex was quantified using an enzyme-linked immunosorbent assay (ELISA) to measure 5-methylcytosine (5-mC) abundance. Datasets for frontal cortical and striatal 5-mC abundance were analyzed by one-way ANOVA with group (F1 $Veh_{n(FCX)=19;\ n(STR)=21}$, F1 $NIC_{n(FCX)=19;\ n(STR)=19}$, or F2 $NIC_{n(FCX)=16;\ n(STR)=20}$) as the sole factor, and, where appropriate, Holm-Sidak's multiple comparisons post-hoc test was applied. ANOVA revealed main effects of DNE on percent 5-mC content in striatum and frontal cortex ($F_{2,57}$ = 7.57; p = 0.0012 and $F_{2,53}$ = 8.15; p = 0.0009, respectively). In both F1 NIC and F2 NIC mice, there were reductions in the percentage of 5-mC in striatum (p = 0.0103 and p = 0.0010, respectively) (Fig. 10A) and frontal cortex (p = 0.0020 and p = 0.0020, respectively) (Fig. 10B) compared to F1 Veh mice. These data indicate global DNA hypomethylation in striatum and frontal cortex of DNE mice.

4. Discussion

Previous studies in humans indicate that *in utero*/prenatal nicotine exposure increases the risk for ADHD in children (Ernst et al., 2001; Linnet et al., 2003; Centers for Disease Control and Prevention, 2011; Knopik et al., 2016b; He et al., 2017; Huang et al., 2018; Marceau et al., 2018). Here, we evaluated the validity of DNE in mice as a model for ADHD-like offspring behavioral phenotypes and associated neurochemical and epigenetic perturbations, and we also assessed the potential multigenerational impacts of DNE on these outcome measures.

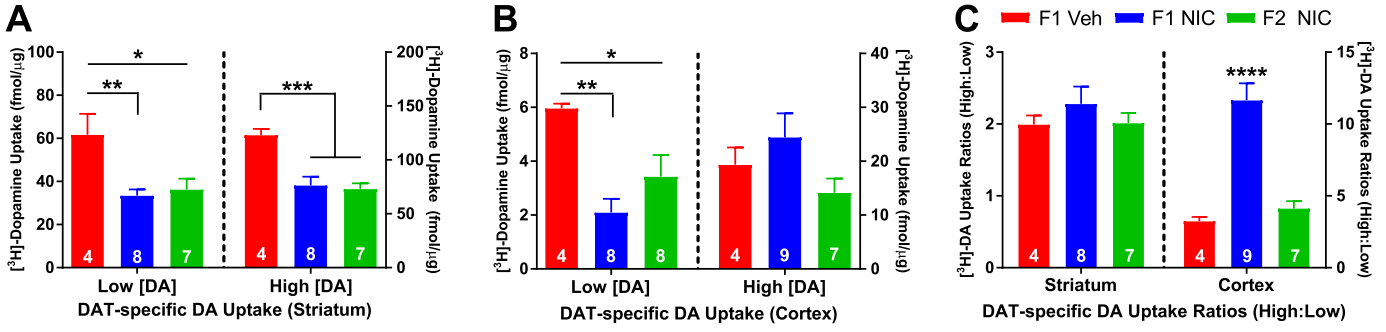

Fig. 9. *Adolescent DNE mice have impaired DAT function in striatum and frontal cortex.* DAT-mediated [^{3}H]-DA uptake in striatum and frontal cortex **(A)** *[^{3}H]-DA uptake at low (left) and high (right) [^{3}H]-DA concentrations in striatum* (n_{F1Veh} = 4, n_{F1NIC} = 8, and n_{F2NIC} = 7). F1 NIC and F2 NIC mice had decreased [^{3}H]-DA uptake at both 0.05 μM [^{3}H]-DA (p = 0.0038 and p = 0.0083, respectively) and 1.0 μM [^{3}H]-DA (p = 0.0002 and p = 0.0001, respectively). **(B)** *[^{3}H]-DA uptake at low (left) and high (right) [^{3}H]-dopamine concentration in frontal cortex* (n_{F1Veh} = 4, n_{F1NIC} = 9, and n_{F2NIC} = 7). F1 NIC and F2 NIC mice had lower [^{3}H]-DA uptake at low (p = 0.004 and p = 0.029, respectively) but not high [^{3}H]-DA concentration in frontal cortex compared to F1 Veh. **(C)** *Ratios of high vs. low concentration [^{3}H]-DA uptake in striatum (left) and frontal cortex (right).* F1 NIC mice had increased high vs. low concentration [^{3}H]-DA uptake ratios in frontal cortex compared to F1 Veh (p = 0.000054) and F2 NIC (p = 0.000018) mice. All data are mean ± S.E.M. *p < 0.05; **p < 0.01; ***p < 0.0001; ****p < 0.0001.

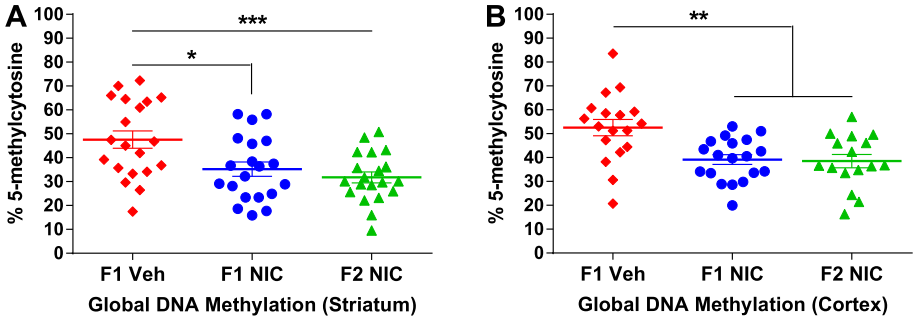

Fig. 10. *Adolescent DNE mice exhibit global DNA hypomethylation in striatum and frontal cortex.* Percent DNA methylation in striatum and frontal cortex, measured by enzyme-linked immunosorbent assay (ELISA). **(A)** *Percent 5-methylcytosine content in striatum* (n_{F1Veh} = 19, n_{F1NIC} = 19, and n_{F2NIC} = 16). F1 NIC and F2 NIC mice had decreased striatal 5-methylcytosine content (p = 0.0103 and p = 0.0010, respectively) compared to F1 Veh mice. **(B)** *Percent 5-methylcytosine content in frontal cortex* (n_{F1Veh} = 21, n_{F1NIC} = 19, and n_{F2NIC} = 20). F1 NIC and F2 NIC mice had decreased cortical 5-methylcytosine content (p = 0.0020 and p = 0.0020, respectively) relative to F1 Veh mice. All data are mean ± S.E.M. *p < 0.05; **p < 0.01; ***p < 0.001.

ADHD is characterized in part by diurnal and nocturnal hyperactivity, sleep disruptions, eveningness, and impulsivity (Van Veen et al., 2010; Baird et al., 2012; Imeraj et al., 2012; American Psychiatric Association, 2013; Bijlenga et al., 2013; Snitselaar et al., 2017). Accordingly, we assessed activity in a familiar (home cage) environment as well as activity and risk-taking behaviors in a novel (open field) environment as proxies for these symptoms. Results indicated that DNE confers multigenerational context-independent hyperactivity and increased risk-taking behaviors. Rhythmometric analyses revealed increases in the midline (MESOR) and the magnitude of daily variation (global amplitude) of home cage activity rhythms in DNE mice that recapitulate findings in ADHD patients (Baird et al., 2012), along with modestly increased latency to peak activity (delayed orthophase) in DNE mice that resembles findings of phase-delayed rest-wake activity rhythms (eveningness) in ADHD patients (Bijlenga et al., 2013). These findings demonstrate ADHD-like anomalies in the rhythmicity of activity that are transmitted to at least the F2 generation.

In light of the associations of both DNE and ADHD with increased nicotine use in adolescents (Cornelius et al., 2000; Buka et al., 2003; Elkins et al., 2018; Rhodes et al., 2016; Kollins et al., 2005; Milberger et al., 1997; Lambert and Hartsough, 1998), we assessed voluntary nicotine consumption and preference in adolescent DNE mice. Results demonstrate a predisposition to voluntary nicotine consumption in both F1 NIC and F2 NIC mice, wherein both generations consumed more nicotine than F1 Veh mice. These findings support previous research demonstrating increased nicotine self-administration in F1 DNE mice (Chistyakov et al., 2010). Interestingly, F1 NIC mice consumed approximately equal volumes of each nicotine concentration, indicating an indifference to the various nicotine solutions, while the volume of nicotine consumed by F2 NIC mice was greatest for the 25 µg/mL concentration and least for the 100 µg/mL concentration. This observation suggests that despite the analogous increases in nicotine consumption in F1 NIC and F2 NIC mice, there appear to be generational differences in sensitivity to nicotine that mimic and extend previous findings in F1 DNE mice (Pauly et al., 2004). The increased nicotine consumption in DNE mice is consistent with the increased risk for nicotine use and dependence in DNE adolescents and ADHD patients (Cornelius et al., 2000; Buka et al., 2003; Gehricke et al., 2009; Elkins et al., 2018; Rhodes et al., 2016; Kollins et al., 2005; Milberger et al., 1997; Lambert and Hartsough, 1998). Furthermore, the phase-delay of home cage activity rhythms at baseline and increased nicotine intake in DNE mice parallels the association of eveningness and smoking (Wittmann et al., 2006). In addition, the increased global amplitude of home cage activity rhythms in DNE mice mirrors the increased in amplitude of rest-wake activity rhythms in ADHD patients. Collectively, the aforementioned results warrant future studies to evaluate the risks for nicotine use and ADHD in the children and the grandchildren of parental smokers.

MPH is an effective treatment for adolescent ADHD patients that mitigates hyperactivity and exerts phase-shifting and MESOR/amplitude-attenuating effects on circadian rest-activity rhythms (Castells et al., 2011; Baird et al., 2012; Storebø et al., 2015; Rezaei et al., 2016; Snitselaar et al., 2017). home cage activity rhythms and open field behavior were thus evaluated during and after passive oral MPH administration to determine the MPH responsivity of ADHD-like hyperactivity, aberrant rhythmicity of home cage activity, and risk-taking behaviors in adolescent DNE mice. Results indicated a therapeutic-like effect of MPH on active and inactive phase home cage hyperactivity and risk-taking behaviors in DNE mice. Similarly, MPH attenuated decreased MESOR and global amplitude of home cage activity rhythms, and elicited an orthophase-advance in DNE mice, consistent with the MESOR/amplitude-attenuating and phase-shifting effects of psychostimulants such as MPH on circadian rest-activity rhythms in ADHD patients (Snitselaar et al., 2017). Conversely, MPH increased home cage and open field activity, risk-taking behaviors, MESOR, global amplitude, and latency to peak activity in F1 Veh mice, consistent with a stimulant-like effect. Interestingly, F1 Veh mice consumed more MPH than DNE mice. In further support of a therapeutic-like effect of MPH, DNE mice displayed negative correlations between daily MPH consumption and active phase home cage activity, inactive phase home cage activity, and risk-taking behaviors, while each of these correlations was positive for F1 Veh mice, consistent with a stimulant-like effect (Fig. S3). Taken together, these findings demonstrate discrete therapeutic-like effects of MPH on hyperactivity, anomalous circadian rhythmicity of activity, and risk-taking behaviors in DNE mice which mimic those produced by MPH in ADHD patients (Castells et al., 2011; Baird et al., 2012; Storebø et al., 2015; Rezaei et al., 2016; Snitselaar et al., 2017) and in other animal models of ADHD (Volkow et al., 2001; Balcioglu et al., 2009; Zhu et al., 2012, 2017). In aggregate, the therapeutic effects of MPH in DNE mice support the construct validity and ADHD specificity of our ADHD mouse model.

Per the self-medication hypothesis of nicotine use in ADHD, a therapeutic effect of nicotine may mediate the increased risk for nicotine dependence in ADHD patients (Gehricke et al., 2009; Amsterdam et al., 2018). home cage activity rhythms and open field behavior were therefore assessed during voluntary nicotine consumption and withdrawal. Consistent with observations in ADHD patients, data indicated a therapeutic-like effect of voluntary nicotine consumption on home cage hyperactivity in the active and inactive phases as well as MESOR and orthophase estimates in DNE mice. In contrast, voluntary nicotine consumption induced active phase home cage hyperactivity and increased MESOR and global amplitude of home cage activity rhythms in F1 Veh mice. In accordance with a therapeutic-like effect of nicotine in ADHD, there were negative correlations between voluntary nicotine consumption and active phase home cage activity during voluntary nicotine intake in DNE mice, while this correlation was positive for F1 Veh mice (data not shown). During withdrawal, F1 NIC mice exhibited a decrease in risk-taking behaviors, which may be reminiscent of the exacerbated withdrawal symptoms reported by nicotine-dependent ADHD patients (Gray et al., 2010; Bidwell et al., 2018). Taken together, these findings support the purported therapeutic effect of nicotine on ADHD symptoms, thereby providing further support for the construct

validity and ADHD specificity of our ADHD mouse model.

Previous research suggests striatal hyperdopaminergia, impaired frontal cortical function, and deficient DAT expression/function in striatum and frontal cortex in ADHD patients and DNE children (Slotkin et al., 1987, Muneoka et al., 1999; Slotkin, 2002; Heath and Picciotto, 2009; Smith et al., 2010; Del Campo et al., 2011; Yochum et al., 2014; Alkam et al., 2017). Prior studies have hypothesized that DNE-induced alterations in corticostriatothalamic nAChR function may constitute a mechanistic link between DNE and ADHD (Heath and Picciotto, 2009). We thus characterized nAChR binding and function and DAT function in striatum and frontal cortex of DNE mice. Indicative of a role for nAChR changes in our DNE mouse model of ADHD, results of binding assays revealed up-regulation of α4β2* nAChR binding sites in striatum of F2 NIC mice, down-regulation of α6β2* nAChR binding sites in striatum of F1 NIC mice, and down-regulation of α4β2 and non-α4β2* nAChR binding sites in frontal cortex of F2 NIC mice. In addition, functional assays revealed nAChR subtype-independent increases in maximal nicotine-induced striatal DA release in DNE mice, accompanied by deficits in frontal cortical α4β2* nAChR function in DNE mice that mirror the frontal cortical dysfunction seen in ADHD and DNE adolescents. Interestingly, the DNE-induced functional impairment of frontal cortical nAChRs appears to be selectively mediated by the α4β2* nAChR population with low sensitivity (LS) to ACh stimulation. This observation suggests that DNE may exert multigenerational effects on both the expression and stoichiometry of frontal cortical α4β2* nAChRs.

DNE was also found to impact DAT function. Analogous to the perturbed DA kinetics and DAT dysfunction in ADHD patients, uptake assays revealed impaired DAT-mediated DA uptake in striatum and frontal cortex of DNE mice, along with increased ratios of high versus low concentration DAT-mediated DA uptake in cortex that suggest an altered DAT K_m in F1 NIC mice alone. In aggregate, the aforementioned results reveal DNE-induced multigenerational perturbations in nAChR expression, dopaminergic and cholinergic function, and DAT function. These findings are consistent with studies in ADHD patients and DNE children demonstrating alterations in corticostriatal dopaminergic and cholinergic signaling that may be associated with changes in nAChR expression/function as well as DAT expression/function (Slotkin et al., 1987, Muneoka et al., 1999; Slotkin, 2002; Heath and Picciotto, 2009; Smith et al., 2010; Del Campo et al., 2011; Yochum et al., 2014; Alkam et al., 2017).

Maternal smoking during pregnancy is associated with DNA methylome alterations in children (Guerrero-Preston et al., 2010; Maccani and Maccani, 2015; Richmond et al., 2015; Jung et al., 2016; Chatterton et al., 2017; Joubert et al., 2016), and DNA methylation levels at birth are negatively correlated with ADHD symptom severity in children (van Mil et al., 2014). Consistent with these studies, our findings indicate DNA methylome deficits in striatum and frontal cortex of not only F1 DNE mice but also F2 DNE mice. By extension, these findings implicate epigenetic changes in the multigenerational transmission of DNE-induced ADHD-like phenotypes, but further research is warranted to elucidate the gene and cell type-specificity of such changes.

There are limitations in the experimental design of this study which should be taken into consideration when interpreting the results. Namely, we cannot rule out possible confounds due to uncontrollable environmental factors such as variations in animal facilities staff. However, care was taken to minimize such confounds through the use of a single experimenter for all behavioral tests, the utilization of standardized climate-control settings for temperature, humidity, and lighting in all animal housing and testing rooms, and the behavioral assessment of a minimum of fifteen litters from twelve breeder pairs for each group. Moreover, multifactorial ANOVAs revealed no main effects of or interactions with breeder, litter, season, or testing chamber for any measure. In addition, it should be noted that, upon co-housing with pre-treated dams, nicotine-naïve sires had the opportunity to consume vehicle or nicotine drinking solutions, and thus our nicotine-exposure paradigm constituted parental rather than exclusively maternal DNE for F1 NIC mice, while F2 NIC mice were exposed to nicotine exclusively via the maternal germline. An additional limitation is the omission of an F2 Veh control group, which confers potential confounds related to the multigenerational transmission of ADHD-like phenotypes in F2 NIC mice. However, pilot experiments revealed no behavioral differences between F1 Veh and F2 Veh mice, and previous research has demonstrated that there are no apparent transgenerational behavioral effects of parental exposure to an oral saccharin vehicle analogous to that used for the present study (Zhu et al., 2012, 2017).

The findings of the present study support the interpretation that DNE elicits multigenerational behavioral, neuropharmacological, and neuroepigenetic anomalies which recapitulate ADHD pathosymptomatology. Nevertheless, it is important to note that many of the phenotypic aberrations displayed by F1 NIC and F2 NIC mice are also consistent with other neuropsychiatric disorders such as schizophrenia and bipolar disorder. Therefore, the findings of this study may have broader implications for understanding the pathosymptomatology of an array of neuropsychiatric disorders.

5. Conclusions

In aggregate, our data demonstrate that DNE elicits multigenerational transmission of nicotine preference, hyperactivity and risk-taking behaviors, aberrant rhythmicity of activity, atypical nAChR expression and function in striatum and frontal cortex, DAT dysfunction in striatum and frontal cortex, and DNA hypomethylation in striatum and frontal cortex. To the best of our knowledge, this report is the first to demonstrate multigenerational ADHD-like enhancement of nicotine preference, MPH-responsive anomalies in the rhythmicity of activity, perturbations in nAChR expression, dopaminergic and cholinergic dysfunction, functional DAT impairment, and DNA methylome deficits in an animal model of ADHD. In isolation, each of these findings is attributable to ADHD and myriad other psychiatric disorders. Despite this potential overlap, the ensemble of phenotypes identified in DNE mice is markedly more reminiscent of ADHD than of any other neuropsychiatric disorder. Specifically, the increased global amplitude and orthophase-delay observed in DNE mice is consistent with ADHD and distinguishes DNE-induced hyperactivity from generalized hyperactivity that is common across a spectrum of neuropsychiatric disorders. Moreover, the therapeutic-like MPH-responsiveness observed in DNE mice is consistent with ADHD, since psychostimulants such as MPH exert therapeutic effects in ADHD patients (Franke et al., 2011; Castells et al., 2011; Baird et al., 2012; Storebø et al., 2015; Rezaei et al., 2016; Snitselaar et al., 2017). Altogether, the findings of the present study contribute to the growing body of research suggesting mechanistic links between DNE and ADHD and provide a foundation for future epidemiological studies evaluating the risks for nicotine use and ADHD in the children and the grandchildren of parental smokers.

Conflicts of interest

The authors declare no competing financial interests.

Acknowledgements

Research support was provided by the National Institutes of Health (R01 DA003194; R21 DA040228; P30 DA015663; T32 DA017637). The authors express gratitude to Dr. Michael J. Marks and Dr. Sharon R. Grady for providing expertise in the conduction and interpretation of pharmacological experiments.

Appendix A. Supplementary data

Supplementary data to this article can be found online at https://

doi.org/10.1016/j.neuropharm.2019.02.006.

References

Abreu-Villaça, Y., Filgueiras, C.C., Manhães, A.C., 2011. Developmental aspects of the cholinergic system. Behav. Brain Res. 221 (2), 367–378.

Agrawal, A., Scherrer, J., Grant, J.D., Sartor, C., Pergadia, M.L., Duncan, A.E., Xian, H., 2010. The effects of maternal smoking during pregnancy on offspring outcomes. Prev. Med. 50 (1–2), 13.

Agulhon, C., Charnay, Y., Vallet, P., et al., 1999. Corrigendum to: distribution of mRNA for the alpha-subunit of the nicotinic acetylcholine receptor in the human fetal brain. Brain Res Mol Brain Res 63, 384.

Ajarem, J., Ahmad, M., 1998. Prenatal nicotine exposure modifies behavior of mice through early development. Pharmacol. Biochem. Behav. 59, 313–318.

Alkam, T., Mamiya, T., Kimura, N., Yoshida, A., Kihara, D., Tsunoda, Y., Aoyama, Y., Hiramatsu, M., Kim, home cage, Nabeshima, T., 2017. Prenatal nicotine exposure decreases the release of dopamine in the medial frontal cortex and induces atomoxetine-responsive neurobehavioral deficits in mice. Psychopharmacology (Berl), Jun 234 (12), 1853–1869.

American Psychiatric Association, 2013. Diagnostic and Statistical Manual of Mental Disorders (5th ed.). Washington, DC.Diagnostic and Statistical Manual of Mental Disorders (5th ed.). Washington, DC.

Amsterdam, J., van der Velde, B., Schulte, M., van den Brink, W., 2018. Causal factors of increased smoking in ADHD: a systematic review. Subst. Use Misuse 53 (3), 432–445.

Bailey, C.D.C., Tian, M.K., Kang, L., O'Reilly, R., Lambe, E.K., 2014. *Chrna5* genotype determines the long-lasting effects of developmental *in vivo*nicotine exposure on prefrontal attention circuitry. Neuropharmacology 77, 145–155. http://doi.org/10.1016/j.neuropharm.2013.09.003.

Baird, A.L., Coogan, A.N., Siddiqui, A., Donev, R.M., Thome, J., 2012. Adult attention-deficit hyperactivity disorder is associated with alterations in circadian rhythms at the behavioural, endocrine and molecular levels. Mol. Psychiatr. 17 (10), 988–995.

Balcioglu, A., Ren, J.Q., McCarthy, D., Spencer, T.J., Biederman, J., Bhide, P.G., 2009. Plasma and brain concentrations of oral therapeutic doses of methylphenidate and their impact on brain monoamine content in mice. Neuropharmacology 57 (7–8), 687–693.

Bidwell, L.C., Balestriari, S., Colby, S., Knopik, V.S., Tidey, J., 2018. Abstinence-induced withdrawal severity among adolescent smokers with and without ADHD: disentangling effects of nicotine and smoking reinstatement. Psychopharmacology 235, 169–178.

Bijlenga, D., Van Someren, E.J.W., Gruber, R., Bron, T.I., Kruithof, I.F., Spanbroek, E.C.A., Kooij, J.J.S., 2013. Body temperature, activity and melatonin profiles in adults with attention-deficit/hyperactivity disorder and delayed sleep: a case–control study. J. Sleep Res. 22, 607–616.

Buka, S.L., Shenassa, E.D., Niaura, R., 2003. Elevated risk of tobacco dependence among offspring of mothers who smoked during pregnancy: a 30-year prospective study. Am. J. Psychiatry 160 (11), 1978–1984.

Button, T., Maughan, B., McGuffin, P., 2007. The relationship of maternal smoking to psychological problems in the offspring. Early Hum. Dev. 83, 727–732.

Cairns, N.J., Wonnacott, S., 1988. [3H](-)nicotine binding sites in fetal human brain. Brain Res. 475, 1–7.

Castells, X., Ramos-Quiroga, J.A., Rigau, D., Bosch, R., Nogueira, M., Vidal, X., Casas, M., 2011. Efficacy of methylphenidate for adults with attention-deficit hyperactivity disorder: a meta-regression analysis. CNS Drugs 25 (2), 157–169.

Centers for Disease Control and Prevention, 2011. Pregnancy Risk Assessment Monitoring System. Atlanta, GA.

Chistyakov, V., Patkina, N., Tammimäki, A., Talka, R., Salminen, O., Belozertseva, I., Galankin, T., Tuominen, R., Zvartau, E., 2010. Nicotine exposure throughout early development promotes nicotine self-administration in adolescent mice and induces long-lasting behavioural changes. Eur. J. Pharmacol. 640 (1–3), 87–93.

Chatterton, Z., Hartley, B.J., Seok, M.H., Mendelev, N., Chen, S., Milekic, M., Rosoklija, G., Stankov, A., Trencevsja-Ivanovska, I., Brennand, K., Ge, Yongchao, Dwork, A., Haghighi, F., 2017. In utero exposure to maternal smoking is associated with DNA methylation alterations and reduced neuronal content in the developing fetal brain. Epigenet. Chromatin 10, 4.

Cornelius, M.D., Leech, S.L., Goldschmidt, L., Day, N.L., 2000. Prenatal tobacco exposure: is it risk factor for early tobacco experimentation? Nicotine Tob. Res. 2, 45–52.

Del Campo, N., Chamberlain, S.R., Sahakian, B.J., Robbins, T.W., 2011. The roles of dopamine and noradrenaline in the pathophysiology and treatment of attention-deficit/hyperactivity disorder. Biol. Psychiatry 69 (12), e145–e157.

Drenan, R.M., Grady, S.R., Steele, A.D., McKinney, S., Patzlaff, N.E., McIntosh, J.M., Lester, H.A., 2010. Cholinergic modulation of locomotion and striatal dopamine release is mediated by α6α4* nicotinic acetylcholine receptors. J. Neurosci. 30 (29), 9877–9889.

Elkins, I.J., Saunders, G.R.B., Malone, S.M., Keyes, M.A., Samek, D.R., McGue, M., Iacono, W.G., 2018. Increased risk of smoking in female adolescents who had childhood ADHD. Am. J. Psychiatry 175 (1), 63–70.

Ernst, M., Moolchan, E., Robinson, M., 2001. Behavioral and neural consequences of prenatal exposure to nicotine. J. Am. Acad. Child Adolesc. Psychiatry 40, 630–641.

Falk, L., Nordberg, A., Seiger, A., et al., 2005. Smoking during early pregnancy affects the expression pattern of both nicotinic and muscarinic acetylcholine receptors in human first trimester brainstem and cerebellum. Neuroscience 132, 389–397.

Franke, A.G., Bonertz, C., Christmann, M., Huss, M., Fellgiebel, A., Hildt, E., et al., 2011. Non-medical use of prescription stimulants and illicit use of stimulants for cognitive enhancement in pupils and students in Germany. Pharmacopsychiatry 44, 60–66.

Gehricke, J.G., Hong, N., Whalen, C.K., Steinhoff, K., Wigal, T.L., 2009. Effects of transdermal nicotine on symptoms, moods, and cardiovascular activity in the everyday lives of smokers and nonsmokers with attention-deficit/hyperactivity disorder. Psychol. Addict. Behav. 23 (4), 644–655.

Grady, S., Marks, M.J., Wonnacott, S., Collins, A.C., 1992. Characterization of nicotinic receptor-mediated [3H]-dopamine release from synaptosomes prepared from mouse striatum. J. Neurochem. 59 (3), 848–856.

Grady, S.R., Moretti, M., Zoli, M., Marks, M.J., Zanardi, A., Pucci, L., Clementi, F., Gotti, C., 2009. Rodent habenulo-interpeduncular pathway expresses a large variety of uncommon nAChR subtypes, but only the alpha3beta4* and alpha3beta3beta4* subtypes mediate acetylcholine release. J. Neurosci. 29, 2272–2282.

Grady, S.R., Salminen, O., Laverty, D.C., Whiteaker, P., McIntosh, J.M., Collins, A.C., Marks, M.J., 2007. The subtypes of nicotinic acetylcholine receptors on dopaminergic terminals of mouse striatum. Biochem. Pharmacol. 74, 1235–1246.

Grady, S.R., Salminen, O., McIntosh, J.M., Marks, M.J., Collins, A.C., 2010. Mouse striatal dopamine nerve terminals express alpha4alpha5beta2 and two stoichiometric forms of alpha4beta2*-nicotinic acetylcholine receptors. J. Mol. Neurosci. 40, 91–95.

Gray, K.M., Baker, N.L., Carpenter, M.J., Lewis, A.L., Upadhyaya, H.P., 2010. Attention-deficit/hyperactivity disorder confounds withdrawal self-report in adolescent smokers. Am. J. Addict. 19 (4), 325–331.

Guerrero-Preston, R., Goldman, L.R., Brebi-Mieville, P., Ili-Gangas, C., Lebron, C., Witter, F.R., Apelberg, B.J., Hernández-Roystacher, M., Jaffe, A., Halden, R.U., Sidransky, D., 2010. Global DNA hypomethylation is associated with in utero exposure to cotinine and perfluorinated alkyl compounds. Epigenetics 5 (6), 539–546.

He, Y., Chen, J., Zhu, L.H., Hua, L.L., Ke, F.F., 2017. Maternal smoking during pregnancy and ADHD: results from a systematic review and meta-analysis of prospective cohort studies. J. Atten. Disord 1087054717696766.

Heath, C.J., Horst, N.K., Picciotto, M.R., 2010. Oral nicotine consumption does not affect maternal care or early development in mice but results in modest hyperactivity in adolescence. Physiol. Behav. 101 (5), 764–769.

Heath, C.J., Picciotto, M.R., 2009. Nicotine-induced plasticity during development: modulation of the cholinergic system and long-term consequences for circuits involved in attention and sensory processing. Neuropharmacology 56, 254–262.

Hellstrom-Lindahl, E., Gorbounova, O., Seiger, A., et al., 1998. Regional distribution of nicotinic receptors during prenatal development of human brain and spinal cord. Brain Res Dev Brain Res 108, 147–160.

Huang, L., Wang, Y., Zhang, L., Zheng, Z., Zhu, T., Qu, Y., Mu, D., 2018. Maternal smoking and attention-deficit/hyperactivity disorder in offspring: a meta-analysis. Pediatrics 141 (1).

Imeraj, L., Sonuga-Barke, E., Antrop, I., Roeyers, H., Wiersema, R., Bal, S., Deboutte, D., 2012. Altered circadian profiles in attention-deficit/hyperactivity disorder: an integrative review and theoretical framework for future studies. Neurosci. Biobehav. Rev. 36 (8), 1897–1919.

Jin, Z., Chen, X.F., Ran, Y., Li, X., Xiong, J., Zheng, Y., Li, Y.F., 2017. Mouse strain differences in SSRI sensitivity correlate with serotonin transporter binding and function. Sci. Rep. 7, 8631. http://doi.org/10.1038/s41598-017-08953-4.

Joubert, B.R., Haberg, S.E., Nilsen, R.M., et al., 2012. 450 K epigenome-wide scan identifies differential DNA methylation in newborns related to maternal smoking during pregnancy. Environ. Health Perspect. 120, 1425–1431.

Joubert, B.R., Felix, J.F., Yousefi, P., Bakulski, K.M., Just, A.C., Breton, C., London, S.J., 2016. DNA methylation in newborns and maternal smoking in pregnancy: genome-wide consortium meta-analysis. Am. J. Hum. Genet. 98 (4), 680–696. http://doi.org/10.1016/j.ajhg.2016.02.019.

Jung, Y., Hsieh, L.S., Lee, A.M., Zhou, Z., Coman, D., Heath, C.J., Hyder, F., Mineur, Y.S., Yuan, Q., Goldman, D., Bordey, A., Picciotto, M.R., 2016. An epigenetic mechanism mediates developmental nicotine effects on neuronal structure and behavior. Nat. Neurosci. 19, 905–914.

Knopik, V.S., 2009. Maternal smoking during pregnancy and child outcomes: real or spurious effect? Dev. Neuropsychol. 34 (1), 1–36.

Knopik, V.S., Marceau, K., Palmer, Rhome cage, Smith, T.F., Heath, A.C., 2016a. Maternal smoking during pregnancy and offspring birth weight: a genetically-informed approach comparing multiple raters. Behav. Genet. 46 (3), 353–364.

Knopik, V.S., Marceau, K., Bidwell, L.C., Palmer, R.H., Smith, T.F., Todorov, A., Evans, A.S., Heath, A.C., 2016b. Smoking during pregnancy and ADHD risk: a genetically informed, multiple-rater approach. Am. J. Med. Genet. B 171B, 971–981.

Knopik, V.S., Marceau, K., Bidwell, L.C., Rolan, E., 2018. Prenatal substance exposure and offspring development: does DNA methylation play a role? Neurotoxicol. Teratol (in press).

Kollins, S.H., McClernon, F.J., Fuemmeler, B.F., 2005. Association between smoking and attention-deficit/hyperactivity disorder symptoms in a population-based sample of young adults. Arch. Gen. Psychiatr. 62 (10), 1142–1147.

Lambert, N.M., Hartsough, C.S., 1998. Prospective study of tobacco smoking and substance dependencies among samples of ADHD and non-ADHD participants. J. Learn. Disabil. 31, 533–544.

Li, X.C., Karadsheh, M.S., Jenkins, P.M., Brooks, J.C., Drapeau, J.A., Shah, M.S., Lautner, M.A., Stitzel, J.A., 2007. Chromosomal loci that influence oral nicotine consumption in C57BL/6J x C3H/HeJ F2 intercross mice. Genes Brain Behav. 6 (5), 401–410.

Linnet, K., Dalsgaard, S., Obel, C., Wisborg, K., Henriksen, T., Rodriguez, A., Kotimaa, A., Moilanen, I., Thomsen, P., Olsen, J., Jarvelin, M., 2003. Maternal lifestyle factors in pregnancy risk of attention deficit hyperactivity disorder and associated behaviors: review of the current evidence. Am. J. Psychiatry 160, 1028–1040.

Logan, R.W., Williams, W.P., McClung, C.A., 2014. Circadian rhythms and addiction: mechanistic insights and future directions. Behav. Neurosci. 128 (3), 387–412.

Maccani, J.Z.J., Maccani, M.A., 2015. Altered placental DNA methylation patterns associated with maternal smoking: current perspectives. Adv. Genom. Genet. (5), 205–214.

Marceau, K., Cinnamon Bidwell, L., Karoly, H.C., et al., 2018. Within-family effects of

smoking during pregnancy on ADHD: the importance of phenotype. J. Abnorm. Child Psychol. 46, 685.
Marks, M.J., Meinerz, N.M., Brown, R.W., Collins, A.C., 2010. 86Rb+ efflux mediated by alpha4beta2*-nicotinic acetylcholine receptors with high and low-sensitivity to stimulation by acetylcholine display similar agonist-induced desensitization. Biochem. Pharmacol. 80, 1238–1251.
Marks, M.J., Meinerz, N.M., Drago, J., Collins, A.C., 2007. Gene targeting demonstrates that alpha4 nicotinic acetylcholine receptor subunits contribute to expression of diverse [3H]epibatidine binding sites and components of biphasic 86Rb+ efflux with high and low sensitivity to stimulation by acetylcholine. Neuropharmacology 53, 390–405.
Marks, M.J., Rowell, P.P., Cao, J.Z., Grady, S.R., McCallum, S.E., Collins, A.C., 2004. Subsets of acetylcholine-stimulated 86Rb+ efflux and [125I]-epibatidine binding sites in C57BL/6 mouse brain are differentially affected by chronic nicotine treatment. Neuropharmacology 46, 1141–1157.
Marks, M.J., Whiteaker, P., Calcaterra, J., Stitzel, J.A., Bullock, A.E., Grady, S.R., Picciotto, M.R., Changeux, J.P., Collins, A.C., 1999. Two pharmacologically distinct components of nicotinic receptor-mediated rubidium efflux in mouse brain require the beta2 subunit. J. Pharmacol. Exp. Therapeut. 289, 1090–1103.
Milberger, S., Biederman, J., Faraone, S.V., Chen, L., Jones, J., 1997. ADHD is associated with early initiation of cigarette smoking in children and adolescents. J. Am. Acad. Child Adolesc. Psychiatry 36, 37–44.
Muneoka, K., Nakatsu, T., Fuji, J., Ogawa, T., Takigawa, M., 1999. Prenatal administration of nicotine results in dopaminergic alterations in the neofrontal cortex. Neurotoxicol. Teratol. 21 (5), 603–609.
National Survey of Children's Health, 2011. Child and Adolescent Health Measurement Initiative (CAHMI), "2011-2012 NSCH: Child Health Indicator and Subgroups SAS Codebook, Version 1.02013, Data Resource Center for Child and Adolescent Health. 2012. .
Pauly, J., Sparks, J., Hauser, K., Pauly, T., 2004. In utero nicotine exposure causes persistent, gender-dependant changes in locomotor activity and sensitivity to nicotine in C57Bl/6 mice. Int. J. Dev. Neurosci. 22, 329–337.
Paz, R., Barsness, B., Martenson, T., Tanner, D., Allan, A., 2007. Behavioral teratogenicity induced by nonforced maternal nicotine consumption. Neuropsychopharmacology 32, 693–699.
Rezaei, G., Hosseini, S.A., Sari, A.A., Olyaeemanesh, A., Lotfi, M.H., Yassini, M., Bidaki, R., Nouri, B., 2016. Comparative efficacy of methylphenidate and atomoxetine in the treatment of attention deficit hyperactivity disorder in children and adolescents: a systematic review and meta-analysis. Med. J. Islam. Repub. Iran 30, 325 2016.
Richmond, R.C., Simpkin, A.J., Woodward, G., Gaunt, T.R., Lyttleton, O., McArdle, W.L., Relton, C.L., 2015. Prenatal exposure to maternal smoking and offspring DNA methylation across the lifecourse: findings from the Avon Longitudinal Study of Parents and Children (ALSPAC). Hum. Mol. Genet. 24 (8), 2201–2217.
Rhodes, J.D., Pelham, W.E., Gnagy, E.M., Shiffman, S., Derefinko, K.J., Molina, B.S.G., 2016. Cigarette smoking and ADHD: an examination of prognostically relevant smoking behaviors among adolescents and young adults. Psychol. Addict. Behav. 30 (5), 588–600.
Salihu, H., Wilson, R., 2007. Epidemiology of prenatal smoking and perinatal outcomes. Early Hum. Dev. 83, 713–720.
Salminen, O., Drapeau, J.A., McIntosh, J.M., Collins, A.C., Marks, M.J., Grady, S.R., 2007. Pharmacology of alpha-conotoxin MII-sensitive subtypes of nicotinic acetylcholine receptors isolated by breeding of null mutant mice. Mol. Pharmacol. 71, 1563–1571.
Salminen, O., Murphy, K.L., McIntosh, J.M., Drago, J., Marks, M.J., Collins, A.C., Grady, S.R., 2004. Subunit composition and pharmacology of two classes of striatal presynaptic nicotinic acetylcholine receptors mediating dopamine release in mice. Mol. Pharmacol. 65, 1526–1535.
Slotkin, T.A., 2002. Nicotine and the adolescent brain: insights from an animal model. Neurotoxicol. Teratol. 24, 369–384.
Slotkin, T.A., Cho, H., Whitmore, W.L., 1987. Effects of prenatal nicotine exposure on neuronal development: selective actions on central and peripheral catecholaminergic pathways. Brain Res. Bull. 18, 601–611.
Smith, A.M., Dwoskin, L.P., Pauly, J.R., 2010. Early exposure to nicotine during critical periods of brain development: mechanisms and consequences. J. Pediatr. Biochem. 1 (2), 125–141.
Snitselaar, M.A., Smits, M.G., van der Heijden, K.B., Spijker, J., 2017. Sleep and circadian rhythmicity in adult ADHD and the effect of stimulants: a review of the current literature. J. Atten. Disord. 21 (1), 14–26.
Storebø, J., Krogh, H.B., Ramstad, E., Moreira-Maia, C.R., Holmskov, M., Skoog, M., 2015. Methylphenidate for attention-deficit/hyperactivity disorder in children and adolescents: cochrane systematic review with meta-analyses and trial sequential analyses of randomised clinical trials. BMJ 351, h5203.
van Mil, N.H., Steegers-Theunissen, R.P., Bouwland-Both, M.I., Verbiest, M.M., Rijlaarsdam, J., Hofman, A., Steegers, E.A., Heijmans, B.T., Jaddoe, V.W., Verhulst, F.C., Stolk, L., Eilers, P.H., Uitterlinden, A.G., Tiemeier, H., 2014. DNA methylation profiles at birth and child ADHD symptoms. Psychiatr. Res. 49, 51–59.
Van Veen, M.M., Kooij, J.J., Boonstra, A.M., Gordijn, M.C., Van Someren, E.J., 2010. Delayed circadian rhythm in adults with attention-deficit/hyperactivity disorder and chronic sleep-onset insomnia. Biol. Psychiatry 67 (11), 1091–1096.
Volkow, N.D., Wang, G., Fowler, J.S., Logan, J., Gerasimov, M., Maynard, L., Ding, Y., Gatley, S.J., Gifford, A., Franceschi, D., 2001. Therapeutic doses of oral methylphenidate significantly increase extracellular dopamine in the human brain. J. Neurosci. 21 (2), RC121.
Whiteaker, P., Jimenez, M., McIntosh, J.M., Collins, A.C., Marks, M.J., 2000. Identification of a novel nicotinic binding site in mouse brain using [(125)I]-epibatidine. Br. J. Pharmacol. 131 (4), 729–739.
Wittmann, M., Dinich, J., Merrow, M., Roenneberg, T., 2006. Social jetlag: misalignment of biological and social time. Chronobiol. Int. 23 (1–2), 497–509.
Yochum, C., Doherty-Lyon, S., Hoffman, C., Hossain, M.M., Zellikoff, J.T., Richardson, J.R., 2014. Prenatal cigarette smoke exposure causes hyperactivity and agressive behavior: role of altered catcholamines and BDNF. Exp. Neurol. 254, 145–152. http://doi.org/10.1016/j.exDNEurol.2014.01.016.
Zhu, J., Fan, F., McCarthy, D.M., Zhang, L., Cannon, E.N., Spencer, T.J., Biederman, J., Bhide, P.G., 2017. A prenatal nicotine exposure mouse model of methylphenidate responsive ADHD-associated cognitive phenotypes. Int. J. Dev. Neurosci. 58, 26–34.
Zhu, J., Zhang, X., Xu, Y., Spencer, T.J., Biederman, J., Bhide, P.G., 2012. A Prenatal nicotine exposure mouse model showing hyperactivity, reduced cingulate frontal cortex volume, reduced dopamine turnover and responsiveness to oral methylphenidate treatment. J. Neurosci. 32 (27), 9410–9418.